Demonstration of micro-grid energy management systems in Gothenburg

Version 3.0

Deliverable 6.1

Kyriaki Antoniadou-Plytaria

01 April 2020

ERA-Net Smart Energy Systems

This project has received funding in the framework of the joint programming initiative ERA-Net Smart Energy Systems, with support from the European Union's Horizon 2020 research and innovation programme.

INTERNAL REFERENCE

- **Deliverable No.:** D6.1
- **Deliverable Name:** Report on Chalmers and GE demonstrations
- **Lead Partner:** Chalmers
- **Work Package No.:** WP6
- **Task No. & Name:** Task 6.1
- **Document (File):** WP6.1 report.docx
- **Issue (Save) Date:** 2020-04-01

DOCUMENT SENSITIVITY

☐	**Not Sensitive**	Contains only factual or background information; contains no new or additional analysis, recommendations or policy-relevant statements
☑	**Moderately Sensitive**	Contains some analysis or interpretation of results; contains no recommendations or policy-relevant statements
☐	**Sensitive**	Contains analysis or interpretation of results with policy-relevance and/or recommendations or policy-relevant statements
☐	**Highly Sensitive Confidential**	Contains significant analysis or interpretation of results with major policy-relevance or implications, contains extensive recommendations or policy-relevant statements, and/or contain policy-prescriptive statements. This sensitivity requires SB decision.

DOCUMENT STATUS

	Date	Person(s)	Organisation
Author(s)	18/03/2020	Kyriaki Antoniadou-Plytaria	Chalmers
Verification by	16/03/2020 25/03/2020	Mohammad Ali Fotouhi Ghazvini Quoc Tuan Tran	Chalmers CEA
Approval by	30/03/2020	Niyam Haque	TU/e

ERA-Net Smart Energy Systems

This project has received funding in the framework of the joint programming initiative ERA-Net Smart Energy Systems, with support from the European Union's Horizon 2020 research and innovation programme.

CONTENTS

Disclaimer

The content and views expressed in this material are those of the authors and do not necessarily reflect the views or opinion of the ERA-Net SES initiative. Any reference given does not necessarily imply the endorsement by ERA-Net SES.

About ERA-Net Smart Energy Systems

ERA-Net Smart Energy Systems (ERA-Net SES) is a transnational joint programming platform of 30 national and regional funding partners for initiating co-creation and promoting energy system innovation. The network of owners and managers of national and regional public funding programs along the innovation chain provides a sustainable and service oriented joint programming platform to finance projects in thematic areas like Smart Power Grids, Regional and Local Energy Systems, Heating and Cooling Networks, Digital Energy and Smart Services, etc.

Co-creating with partners that help to understand the needs of relevant stakeholders, we team up with intermediaries to provide an innovation eco-system supporting consortia for research, innovation, technical development, piloting and demonstration activities. These co-operations pave the way towards implementation in real-life environments and market introduction.

Beyond that, ERA-Net SES provides a Knowledge Community, involving key demo projects and experts from all over Europe, to facilitate learning between projects and programs from the local level up to the European level.

www.eranet-smartenergysystems.eu

List of acronyms

BESS	Battery Energy Storage System
BIMG-EMS	Building-integrated Micro-grid Energy Management System
BMS	Battery Management System
DMS	Distribution Management System
DSO	Distribution System Operator
DoD	Depth-of-Discharge
EMS	Energy Management System
M2M	Machine-to-Machine
MG	Micro-grid
MG-EMS	Micro-grid Energy Management System
MQTT	Message Queuing Telemetry Transport
PCC	Point of Common Coupling
PLC	Power Line Communication
PV	Photovoltaic
RH	Rolling Horizon
SOC	State-of-Charge
SOH	State-of-Health
TCP/IP	Transmission Control Protocol/Internet Protocol

1. Introduction

The m2M-Grid project has developed interfaces for the short-term and real-time operation of micro-grids (MG). The MG operation interfaces can be classified into three categories: 1) *MG control*: to control the MG resources/components by the MG operator, 2) *MG to distribution management system (DMS) coordination*: to control the MG resources (and possibly main grid components) by coordination between the MG operator and the distribution system operator (DSO), and 3) *MG to MG coordination:* to manage the MG resources/components involved in the interaction between the MGs (e.g., energy trading, load sharing).

MGs are defined as clusters of distributed energy sources (generation, storage, flexible loads, etc.) and energy consumers (non-flexible load). The MGs can operate either in grid-connected or in island mode and many MGs can support seamless transition between the two modes to increase supply reliability for the customers. In grid-connected mode, the difference between the MG generation and consumption can be imported or exported to the main grid. In island mode, the MG is completely autonomous meaning that energy is supplied exclusively from the MG resources and any excess in generation must be stored or curtailed, if self-consumption is not an option.

Regardless of the mode of operation, MGs can be considered as controllable entities separate from the main grid because they operate based on their own strategies and objectives. The MG energy sources are managed by the MG operators to supply the consumers in a secure, efficient, and economical way.

If the MG resources/loads can form a network structure or represent a single network component (act as one resource/load), then the MGs are called physical MGs. Otherwise, the clustering of the resources is driven by commercial purposes; this is the case of commercial MGs. The physical MG interfaces were the main topic of Work Package 4 of the m2M-GRID project, while commercial MG interfaces were presented in Work Package 5.

This report describes the demonstration of a MG energy management system (MG-EMS) at two physical test sites in Sweden. The MG-EMS is employed by the MG controller, which manages the clusters of producing and consuming units, and its main task is to optimally balance load and supply (either by MG resources or through interconnections). The MG-EMS and the first demonstration of the MG-EMS at a real-site was first presented in the report for Task 4.3. The work performed for Task 6.1 extends that work and validates the developed MG-EMS at the test systems, which were set up at the demo sites.

1.1 Objectives

MGs can be employed at various locations including both rural and urban areas. Off-grid solutions are usually ideal for remote rural areas. In cities, on the other hand, grid-connected MGs can be formed by clusters of distributed energy resources that are integrated in commercial or residential buildings. A MG can consist of a number of buildings and often it can be the building itself that integrates a MG-EMS, so that the management of its installed resources can be in tight relation with the the building load consumption. These type of MGs have been defined as building MGs or building-integrated MGs [1]-[2].

The purpose of the site tests is to evaluate the performance of energy scheduling algorithms implemented by building-integrated MG energy management systems (BIMG-EMS). The main objectives of the physical site demonstrations are:

- To validate the compatibility of different battery energy storage systems (BESS) models with the actual operation of the on-site BESS.
- To discuss the benefits and shortcomings of the developed BESS models and describe the conditions under which they can reliably be used for scheduling the battery operation.

- To evaluate the performance of the energy scheduling algorithms, when different BESS are used.
- To investigate the possibility of flexibility services and potential value for the MG operators and the distribution system operator (DSO).
- To validate that the BESS can provide battery power flexibility after agreement with the DSO.

The performance metrics of the demonstrations include:

- Energy cost of the microgrid.
- State-of-charge (SOC) profile
- Dispatched battery power
- Feasible amounts and price of battery flexibility

1.2 Outline of the report

The remainder of this report is structured as follows:

- Section 2 introduces the demonstration sites.
- Section 3 describes the characteristics of the test cases.
- Section 4 explains the communication and control setup.
- Section 5 presents the test results and the evaluation of the performance of the proposed algorithms.
- Section 6 concludes and discusses future work.

2. Demonstration sites

Two energy flexible buildings located in Gothenburg, Sweden, were used as demonstration sites for the developed BIMG-EMS.

2.1 Brf Viva

The Brf Viva is a housing association of six buildings, which is in Guldheden, an area close to the Chalmers campus. The buildings consist of 132 residences inhabited since 2018 [6]. In 2019, the building electricity consumption was 162 MWh, and the local energy production of the solar panels was 72 MWh, out of which 11 MWh was exported to the grid. The installed capacity of the photovoltaic (PV) systems is 170.8 kWp.

In addition, second-life Li-ion batteries taken from old electric buses (provided by Volvo Buses) have been installed (Figure 1 and Figure 2). There are in total 14 batteries, each with a rated capacity of about 14 kWh and a maximum charge/discharge power of 6 kW. The PV systems and the batteries form a DC grid, which is connected to the upstream AC grid (400 V) via a converter provided by Ferroamp company [5]. The converter (capacity of 168 kVA) is called EnergyHub. It is a multi-level converter with bi-directional operation, since the solar energy and the battery stored energy can be exported to the upstream AC grid and, in addition, the batteries can be charged through the upstream AC grid.

Figure 1 : The second life Li-ion batteries of Brf Viva.

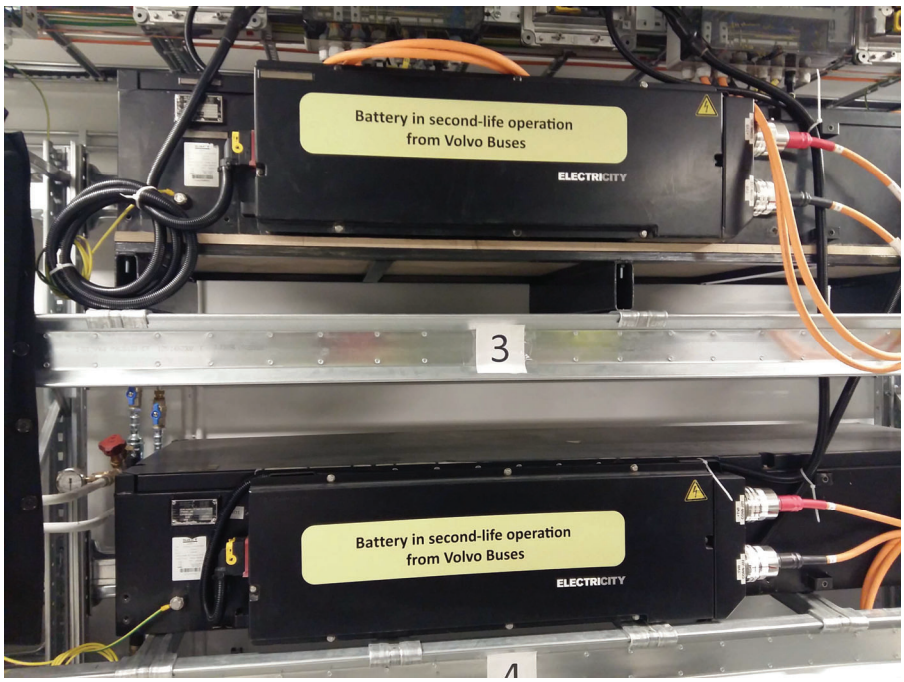

Figure 2 : Second life Li-ion batteries of Brf Viva.

2.2 HSB Living Lab

Inside the Chalmers campus area, there is a multi-family residential building of 29 apartments (Figure 3), which is called HSB Living Lab (HSB LL) [3]-[4]. This building also serves as a testbed for sustainable living solutions, where the living lab approach focuses on applying innovation in human-centred systems. Solar panels are installed on the rooftop and facade. The 18 kWp PV system is coupled with a 7.2 kWh battery, which can be charged both from the PVs and the AC grid. The PV and BESS are connected to the AC grid via a converter provided by the Ferroamp company [5].

Figure 3 : The facade of the HSB LL building.

3. Description of test cases

Two test cases are chosen to evaluate the performance of BIMG-EMS. In demonstration case 1 (DemoCase1), the BIMG-EMS determines the optimal battery scheduling that minimises the energy cost for the MG operator. In demonstration case 2 (DemoCase2), the BIMG interacts with the DSO and provides flexibility services to alleviate the congestion in the upstream grid.

3.1 Demonstration case 1

In Democase1, the BIMG-EMS implements an optimal battery scheduling algorithm that minimizes the energy cost of the building. The optimal battery energy scheduling algorithm was validated in three different tests and was also compared to a rule-based algorithm for battery scheduling. The description of the different tests of DemoCase1 can be seen in Table 1.

Table 1 : Description of tests for DemoCase1

Test #	Description
D1.A	Rule-based algorithm
D1.B	Energy cost minimization algorithm with ideal BESS model
D1.C	Energy cost minimization algorithm with non-ideal BESS model
D1.D	Energy cost and battery degradation cost minimization algorithm with non-ideal BESS model

Battery scheduling demonstrations using a rule-based [4] and an optimization algorithm were performed in HSB LL in April and July 2019, respectively. The results were documented in the report WP4.3 of the m2M-GRID project [7]. The BESS model used in those demonstrations was further improved to account for non-linear battery behaviour due to dependency of delivered charging/discharging power rates and efficiencies to the SOC. As a result, advanced, data-driven models, parametrized with the use of field test data, were developed and validated with demonstrations at each test site.

3.1.1 Rule-based algorithm

The rule-based algorithm tries to constrain the power exchange with the grid between a peak and a low load threshold (P_{peak} and P_{low}, respectively), which can be externally set by the BIMG operator. The purpose of this test is to reduce the peak load consumption as well as to even out the aggregated power profile as seen by the DSO at the point of common coupling (PCC). The algorithm updates the battery output set-point per iteration i based on the average PCC power exchange (P_i^{PCC}) of the previous iteration loop.

The calculation of the charging/discharging battery power set-points (P_i^- / P_i^+) are based on the ideal BESS model, where the SOC of the end of each iteration is linearly dependent on the energy stored in the BESS at the beginning of the iteration and the cumulative throughput during the iteration loop. The discharging/charging power limits P_{max}^- / P_{max}^+ as well as the charging/discharging efficiencies are constant and independent of the SOC level. The SOC level is limited between SOC_{min} and SOC_{max} to avoid deep discharges/charges of the battery.

Algorithm 1, presented in Figure 4, describes the proposed rule-based algorithm.

Algorithm 1: Rule-based battery dispatch algorithm

while $i \leq iter_{max}$ **do**

  Read P_i^{PCC} and $\mathrm{SOC_i}$;

  Calculate P_i^+/P_i^- so that $P_{low} \leq P_i^{PCC} \leq P_{peak}$;

  if $P_i^+/P_i^- > P_{max}^+/P_{max}^-$ **then**

    $P_i^+/P_i^- = P_{max}^+/P_{max}^-$;

  end

  if $(SOC_{i+1} > SOC_{max}) \vee (SOC_{i+1} < SOC_{min})$

  Reduce P_i^+/P_i^- so that $SOC_{min} \leq SOC_{i+1} \leq SOC_{max}$;

  end

  Send P_i^+/P_i^- ;

end

Figure 4 : The rule-based battery dispatch algorithm.

3.1.2 Energy cost minimization with ideal BESS model

The objective function for the BIMG-EMS is

$$max \sum_{t \in T} (c^{spot} + c_e)\, P_t^{ex} \Delta t - (c^{spot} + c_i) P_t^{im} \Delta t - R^p \tag{1}$$

where the first term is the income from selling energy to an electricity energy trader, the second term is the imported energy cost (where network charges are included), and the third term is the cost due to the grid charge for peak imported power.

In (1), T is the simulation horizon, and Δt is the time discretization step. The positive variables P_t^{im}/P_t^{ex} denote the BIMG imported/exported power from/to the main grid. The parameter c^{spot} is the electricity market spot price, c_i is the grid charge for energy transmission, when the BIMG imports energy, and c_e is the reimbursement paid to the BIMG by the DSO (as an incentive to reduce network losses), when the MG exports energy. Finally, R^p is the cost for the peak power (based on the average values measured for each Δt) drawn from the main grid, which must be constrained by

$$R^p \geq C_{pp}^{MG} P_t^{im} \tag{2}$$

where C_{pp}^{MG} denotes the power-based grid tariff.

The active power balance of each BIMG is given by

$$P_t^{PV} + P_t^- + P_{i,t}^{im} = P_t^L + P_t^+ + P_t^{ex}, \quad t \in T \tag{3}$$

Constraint (3) defines the active power balance, where P_t^{PV}, P_t^L, and P_t^+/P_t^- refer to PV generation, load, charging/discharging power from the BESS.

The ideal BESS model is given by the following equations:

$$SOC_t = SOC_{t-1} + \eta_{ch} \frac{P_t^+}{E_{max}} - \frac{P_t^-}{\eta_{dis} E_{max}}, \qquad t \in T \tag{4}$$

$$SOC_{min} \leq SOC_t \leq SOC_{max}, \qquad t \in T \tag{5}$$

$$0 \leq P_t^+ \leq \kappa E_{max}, \; 0 \leq P_t^- \leq \kappa E_{max}, \qquad t \in T \tag{6}$$

$$P_t^+ \leq z_t M, \quad P_t^- \leq (1 - z_t) M, \; t \in T \tag{7}$$

The power to energy ratio, which depends on the energy storage technology and limits the maximum charging or discharging power is denoted by κ, while η_{ch}/η_{dis} is the charging/discharging efficiency, E_{max} is the installed capacity and SOC_t is the SOC, which must lie between the lower and upper limit (SOC_{min} and SOC_{max}), respectively. The binary variable z_t is used to avoid optimal solutions that yield simultaneous charging and discharging battery power set-points, and M is a very large number, which is used to linearize the BESS model. The linearization technique used in this model is called the big-M approach [8].

3.1.3 Energy cost minimization with advanced BESS models

A linear, data-driven model for non-ideal BESS was developed to improve the accuracy of the precious ideal model. The non-ideal data-driven BESS (NIDD-BESS) model was first presented in [9] and uses sample points of SOC and battery power for its parametrization. In Test D1.B, where the ideal BESS model was used, the battery charging/discharging efficiencies and power rate limits are considered constant and independent of SOC levels. In Test D1.C, where the advanced NIDD-BESS model was used in the energy cost minimization algorithm, the charging/discharging efficiencies and power rate limits are dependent on the SOC level. Hence, the advanced, data-driven model represents more accurately the battery behaviour. The parameters are customized for each BESS with sample data from preliminary experiments.

In Test D1.D, the advanced data-driven model was combined with a battery degradation model, which is presented in [10].

3.2 Demonstration case 2

In Democase2, the BIMG-EMS of two energy flexible buildings interact with the DSO. It is assumed that one transformer in the upstream grid trips, which results in the overloading of the other transformer, which is connected in parallel (see Figure 5). For this purpose, the DSO asks for maximum flexibility (power reduction) that can be provided by the grid-connected BIMGs.

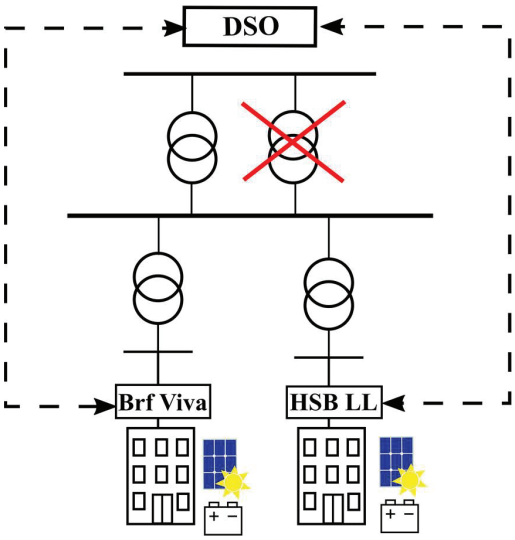

Figure 5 : Simplified diagram of the upstream grid showing the tripping of one transformer.

Each BIMG implements the energy cost minimization algorithm, which was presented in Section 3.1.2 with the time-scale of 1 hour and decides on the battery power dispatch for the next hour. It is assumed that before the set-points are applied, a flexibility request is received from the DSO. The MG then calculates the feasible flexibility amounts it can provide and responds with a curve of flexibility amounts and the price it requests for each flexibility amount. The price is the difference between the optimal cost (derived from the solution of the energy cost minimization problem) and the cost of that the dispatch of the respective flexibility amount yields. The DSO then clears the market and assigns the desired flexibility amount to each BIMG.

4. Communication and control set up

The communication set-up (seen in Figure 6) is the same for both demonstration sites. The BIMG-EMS of each building synchronizes its operation with sensors and controllers using backend services. The Message Queue Telemetry Transport (MQTT) protocol, which runs on top of Transmission Control Protocol/Internet Protocol (TCP/IP), is used for real-time data sharing between the server and the EnergyHub converter of each energy flexible building. The server implements the developed BIMG-EMS and each BIMG-EMS interacts with the measurement and control systems embedded in the respective converter. This is how the BIMG-EMS receives real-time measurements as input for the the battery scheduling algorithm and sends commands (battery power set-points) to the converter. The MQTT protocol is a "machine-to-machine (M2M)/"Internet of Things" connectivity protocol [11], which was designed for lightweight and low power message transport and therefore is very useful for remote control applications.

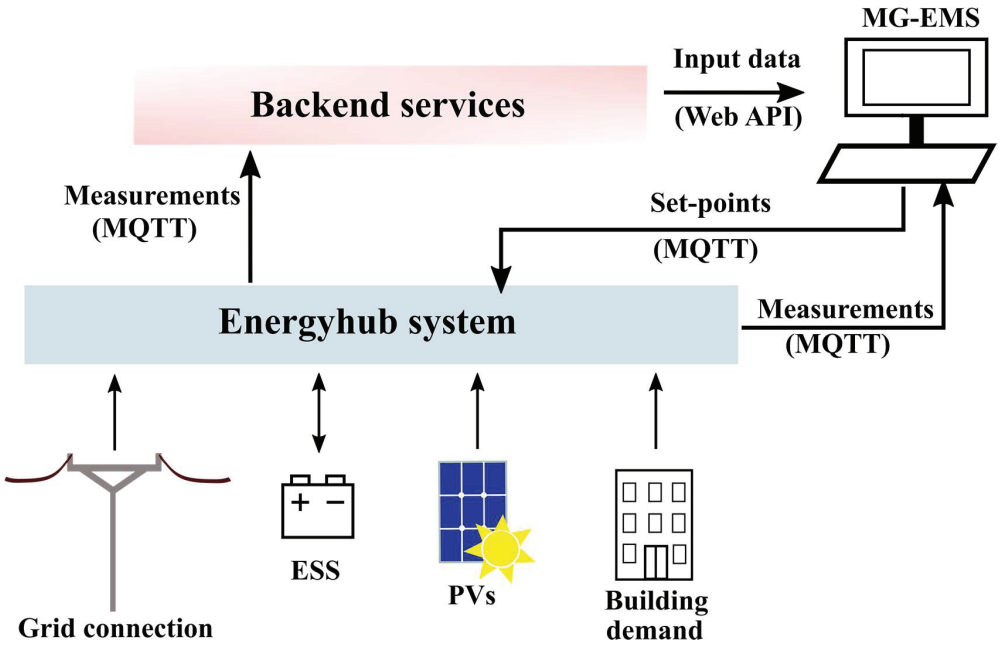

Figure 6: Communication and control interface set-up of the BIMG-EMS.

The data exchange with MQTT is very fast, and the control set-points were received by the broker in about 50-200 msec (from measurements with the HSB LL BIMG-EMS the average response was 130 msec). The process of the command by the converter controller of the PV and BESS system took 10 sec. After that, the control signal was transmitted to the battery DC/DC converter through power line communication (PLC), which adds a small delay to the transmission of the set-point. Once the battery management system (BMS) was actuated, the set-point was reached in about 10 sec depending on the battery status and the amount of requested power. The results for both on-site BESS showed a total delay of 30-40 sec (for more information see Section 5), which means that these remote control systems could be employed by a BIMG-EMS that performs optimization-based energy scheduling with e.g., a 5-minute time scale.

The server has an interface with MATLAB to set up the communication interface with the test site and implement the battery scheduling algorithms. An MQTT publisher/subscriber is built in MATLAB to interact with the MQTT broker run at each EnergyHub. The MATLAB subscriber reads real-time measurements that the MQTT broker transmits in different topics. The MATLAB publisher sends control commands (battery power requests) to the MQTT broker, which will then communicate these requests to the

DC/DC converters of the batteries. In addition to the MQTT protocol, HTTP requests are used to retrieve historical data, which are stored in an SQL-database.

A MATLAB to GAMS interface was used for data exchange with the optimization models and to retrieve the battery scheduling solution (control set-points) that were applied in an online manner. For DemoCase2, a MATLAB to Python interface is used to obtain the solution of the flexibility market clearing (the market is simulated in Python). The design of the communication platform and all the server interfaces that are employed for the demonstrations can be seen in Figure 7.

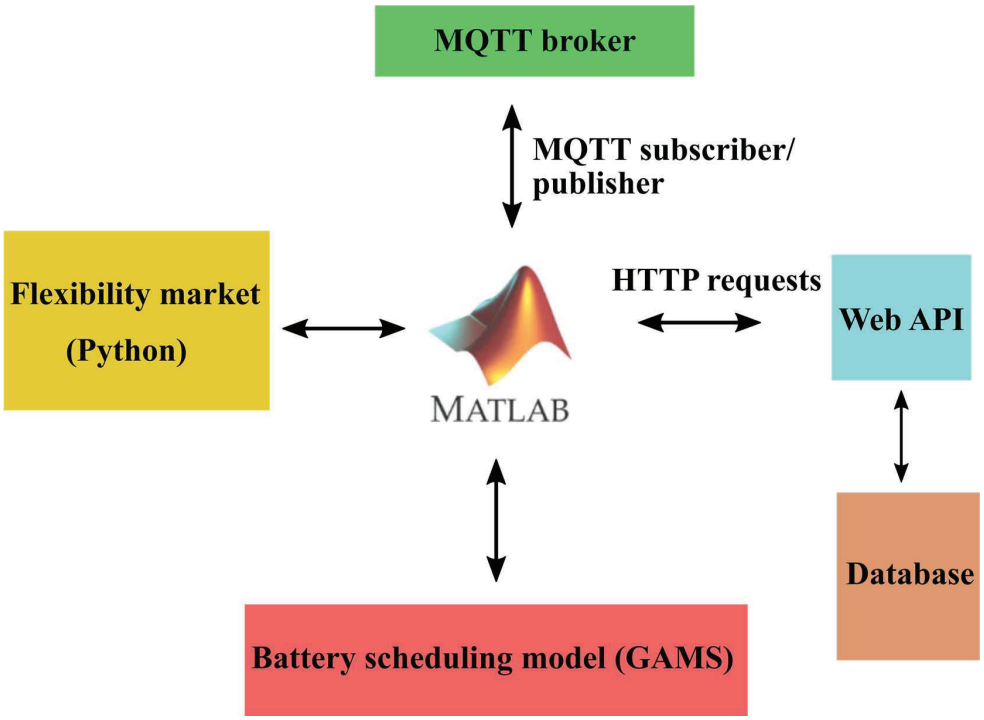

Figure 7 : Design of the communication platform.

5. Performance evaluation

5.1 DemoCase1 in Brf Viva

5.1.1 Demonstration results for preliminary Test D1.B

The energy cost minimization algorithm with the ideal BESS model (Test D1.B of DemoCase1) was first demonstrated in Brf Viva in December 2019. Only four out of fourteen second-life Li-ion batteries were available during the test.

The battery scheduling simulations (solution of the energy cost minimization algorithm) were performed in a rolling horizon (RH) approach. Each simulation had a scheduling horizon of one hour and a time discretization step of 5 min. The energy cost minimization algorithm was solved iteratively every 5 min, so 12 simulations were required to dispatch the battery power set-points of one hour. The commands to the BESS and the input to the algorithm were updated after each iteration. The input included the measured SOC, the spot market price, and the load and PV forecast for the simulation horizon. In this test, historical load and PV data were used as pseudo measurements for the load and PV forecast.

The first series of tests validated that the charging/discharging power requests sent from the BIMG-EMS are followed by the BESS (see Figure 8), and the average communication delay was found to be 40 sec, which was taken into consideration to dispatch the battery power commands accordingly.

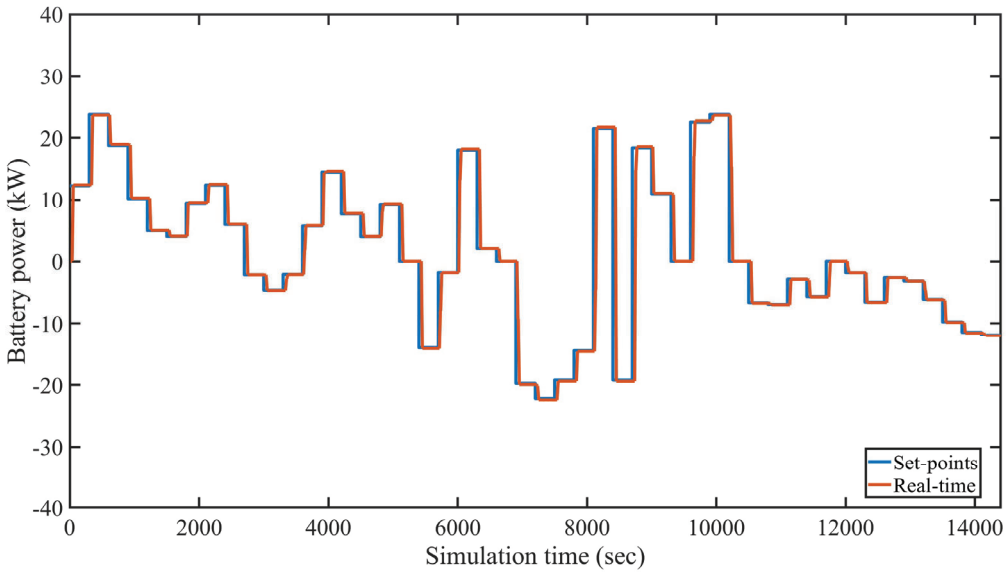

Figure 8 : The set-points and real-time measurements of the battery system power in Brf Viva (Democase1, Test D1.B at 03-12-2019 assuming 100% roundtrip efficiency).

5.1.2 Simulation results for Tests D1.A-D1.D

The simulation results for Tests D1.A-D1.D in Brf Viva gave the battery power dispatch and the SOC estimation given in Figure 9-Figure 12. The simulations of Test D1.B-D1.D are performed in a RH approach with a time horizon of one day and a time discretization step of 5 minutes. One day-ahead simulation was performed every 5 minutes and then the input to the algorithm was updated and the next simulation was performed. A total of 288 simulations was needed to dispatch the battery set-points for the day. The input to the energy cost minimization algorithm of Tests D1.A-D1.D was the forecast profile of the building load and PV generation as well as the electricity spot market and the battery SOC.

The rule-based algorithm (Test D1.A) also required 288 simulations, as the time resolution was 5 min, but no day-ahead scheduling and rolling horizon approach was needed. In every simulation, the input to the algorithm was the battery SOC and the average load consumption and PV generation of the past 5 minutes. The load and PV generation input values to Test D1.B-D1.D were pseudo measurements (derived from historical load and PV data and appropriately added noise) that created a forecast profile of the actual values.

The battery power dispatch in Figure 9 and the SOC profile in Figure 10 show that the battery is cycled more in the case of energy cost minimization, as the battery power follows the fluctuations in spot price. The electricity price used as input for the simulation can be seen in Table 2, where the hours refer to the simulation time and not the actual hours of the day. Small variations in the battery power (e.g., between time step 100 and time step 150) can be attributed to the fact that in each simulation the forecast of the load and the PV generation is updated, which makes the algorithm re-adjust the charging or discharging rate. Bigger variations in battery power are a result of the spot price difference, since the BIMG maximizes the profit through energy arbitrage. This can be observed, e.g., in the first four hours of the simulation (time steps 0-48), where there are big changes in the spot prices for each hour.

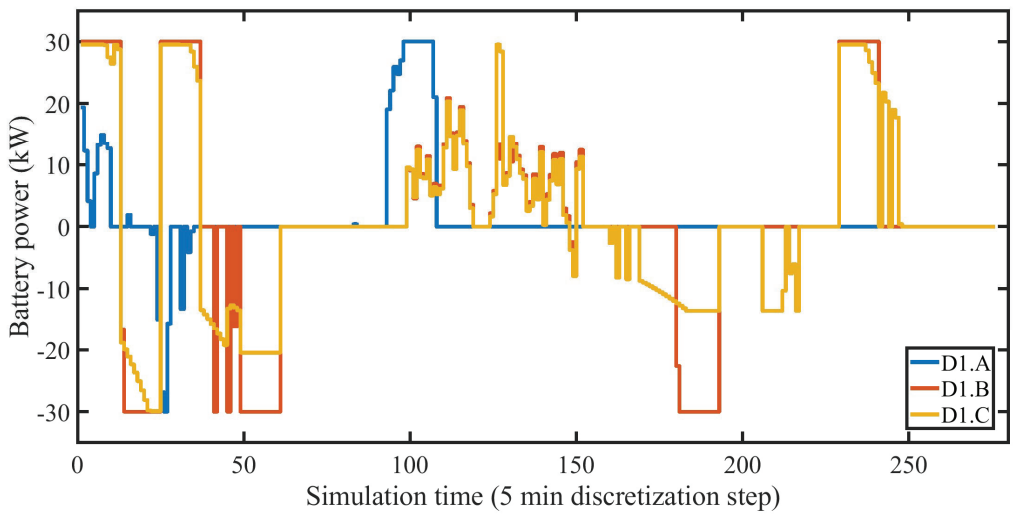

Figure 9 : The battery power dispatch according to the different algorithms in Tests D1.A-D1-C (simulation results).

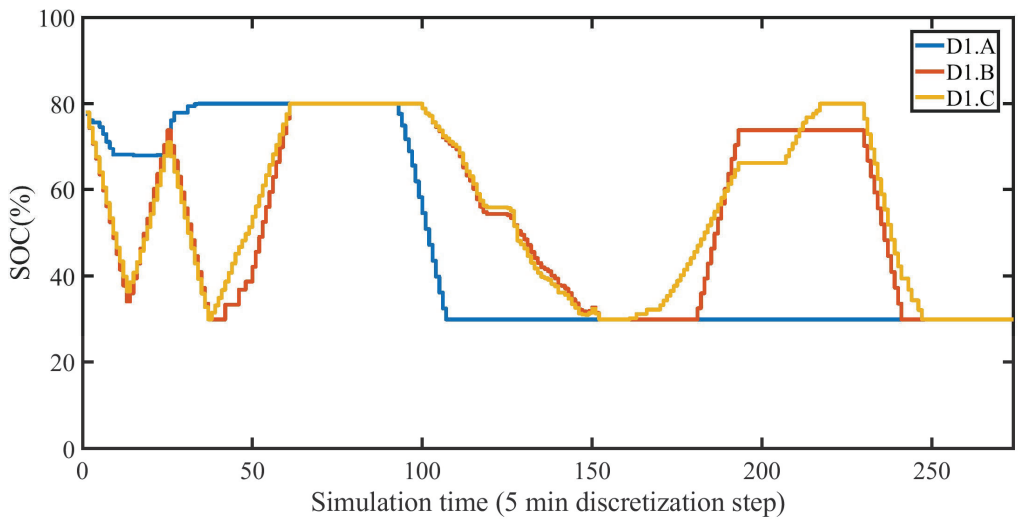

Figure 10 : The estimation of the SOC to the different algorithms in Tests D1.A-D1-C (simulation results).

Table 2 : Spot market electricity prices

Hour	1	2	3	4	5	6	7	8
Price (SEK/MWh)	123.37	54.29	115.84	51.05	42.7	79.48	112.24	122.07
Hour	9	10	11	12	13	14	15	16
Price	134.01	147.44	149.13	140.78	138.56	137.4	135.81	134.96

(SEK/MWh)								
Hour	17	18	19	20	21	22	23	24
Price (SEK/MWh)	137.4	136.76	144.48	149.23	148.60	145.11	136.76	129.15

There is only a small difference in the battery scheduling, when the ideal BESS and the NIDD-BESS models are used, as can be seen from their SOC profiles (Figure 10 and Figure 12). When battery degradation is considered, however, there is a trade-off between the profit from energy arbitrage and cost of battery degradation, which results in the battery dispatch and SOC profile, seen in Figure 11-Figure 12. The loss of battery capacity is affected by both the number of battery cycles and the maximum depth-of-discharge (DoD), so even when the battery is cycled in the first hours, it does not reach the low SOC value of Tests D1.B-C. Moreover, the battery is not cycled once more during the second half of the simulation period (as it happens in Tests D1.B-C) because the profit from energy arbitrage is very small and does not compensate for the cost of lifecycle loss of the battery.

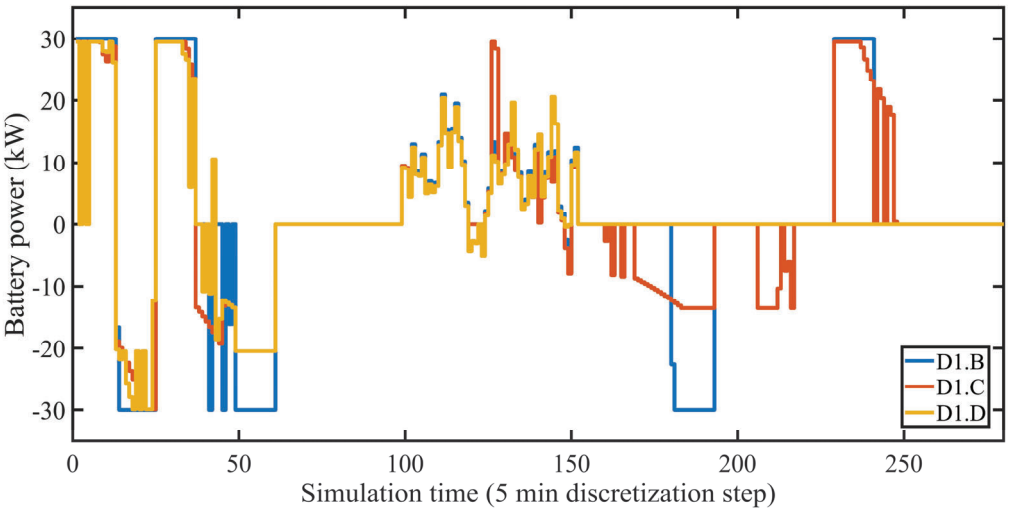

Figure 11 : The battery power dispatch according to the different algorithms in Tests D1.B-D1-D (simulation results).

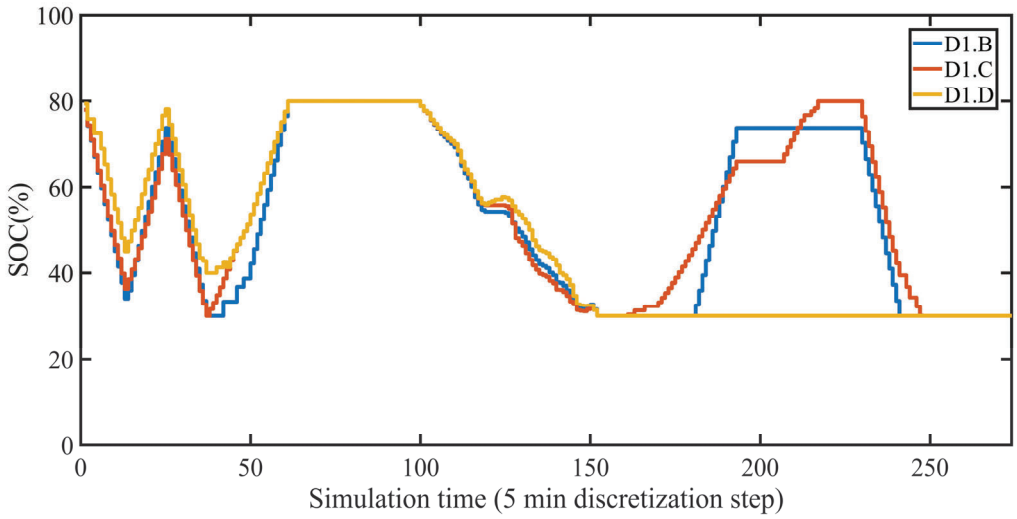

Figure 12 : The estimation of the SOC in Tests D1.B-D1-D (simulation results).

The total cost of BIMG, which consists of the energy and peak power cost can be seen in Table 3. The cost is calculated as described in [12] with a scheduling period of one day; however, the peak power is calculated based on the 5min average of imported power. Since Tests D1.B-D1.D implemented a cost minimization algorithm both the estimated cost from the algorithm and the actual cost is given.

The deviation between the estimated and the actual cost is due to mismatches in generation and consumption attributed to the forecast error. Same applies for the results in Table 4. The realized PV generation and load consumption is assumed for the calculation of actual cost and actual peak. For all metrics, it is assumed that the optimal decisions are accurate (delivered battery power matches the set-points and SOC at the end of each scheduling time-step matches the estimated SOC of the simulation). The accuracy of the solutions will be validated with demonstrations.

Table 3 : The daily cost (in SEK) of BIMG according to simulation results for DemoCase1

Test #	**Estimated cost (forecast error)**	**Actual cost**	**Scheduling with RH (perfect forecast)**
D1.A	—	**625.4 SEK**	—
D1.B	603.6 SEK	605.4 SEK	604.7 SEK
D1.C	603.8 SEK	606.4 SEK	603.9 SEK
D1.D	604.4 SEK	606.6 SEK	606.2 SEK

Table 4 : The daily peak power (in kW) according to simulation results for DemoCase1

Test #	**Estimated peak (forecast error)**	**Actual peak**	**Scheduling with RH (perfect forecast)**
D1.A	—	**152.2 kW**	—

D1.B	131.8 kW	131.9 kW	131.4 kW
D1.C	132.9 kW	132.9 kW	131.2 kW
D1.D	132.5 kW	132.6 kW	132.3 kW

The cost and peak power are higher in the case of rule-based algorithm (Test D1.A); however they could be different depending on the choice of the peak and low load threshold (in this case it was 85 kW and 50 kW, respectively). Since there is no forecast of the load consumption and the battery dispatch is dependent on the grid power exchange of the past 5 minutes, it is hard to capture and reduce the peak power. This algorithm uses the battery in a non-optimal way, as the battery energy storage levels might be depleted, when the daily peak power occurs. This problem can be observed in Figure 9-Figure 10, where there is big discharge power rate applied by the rule-based algorithm starting at time-step 100, whereas the cost minimization algorithms apply a more conservative battery scheduling, saving energy for the expected peak power.

From the results of Test D1.D, one can observe the trade-off between energy arbitrage and battery degradation. The cost of battery degradation, which is applied in Test D1.D, penalizes deep discharges. In this test, however, the BIMG can profit a lot from energy arbitrage in the first 4 hours, which is why the battery scheduling is very similar to Test D1.B and Test D1.C, although with not as deep discharges. Unlike Tests D1.B-C, though, the battery is not cycled towards the end-of the day because the gain from energy arbitrage is small compared to battery degradation cost. The gain is in fact that small, that the total cost is practically similar in Tests D1.B-D.

5.1.3 Demonstration results for Tests D1.A-D1.D

The exact same input that was used in simulation was also used for the real-site application of Tests D1.A-D1.D. Specifically, the same load consumption and PV generation that was used in simulation was also used in demonstration of Test D1.A and then the same "forecasted" load and PV generation as well as electricity price that were used in simulated Tests D1.B-D1.D were used for the demonstration of these tests. During the real-site tests, however, the SOC of the BESS was read online and the input to the algorithm was updated from the real-time measurement and not from the solution of the algorithm, as was done in simulation.

Experimental measurements from preliminary tests were used to parametrize the BESS models. For the ideal BESS model (Tests D1.A-B), the average charging and discharging efficiency from the experimental measurements were used, which was 97% both for charging and discharging. This section presents the results of the final demonstrations of Tests D1.A-D1.D in Brf Viva. For this series of tests, five out of the fourteen second-life Li-ion batteries were available for the validation of the battery scheduling algorithms.

The results of Test D1.A (rule-based algorithm) can be seen in Figure 13-Figure 15.

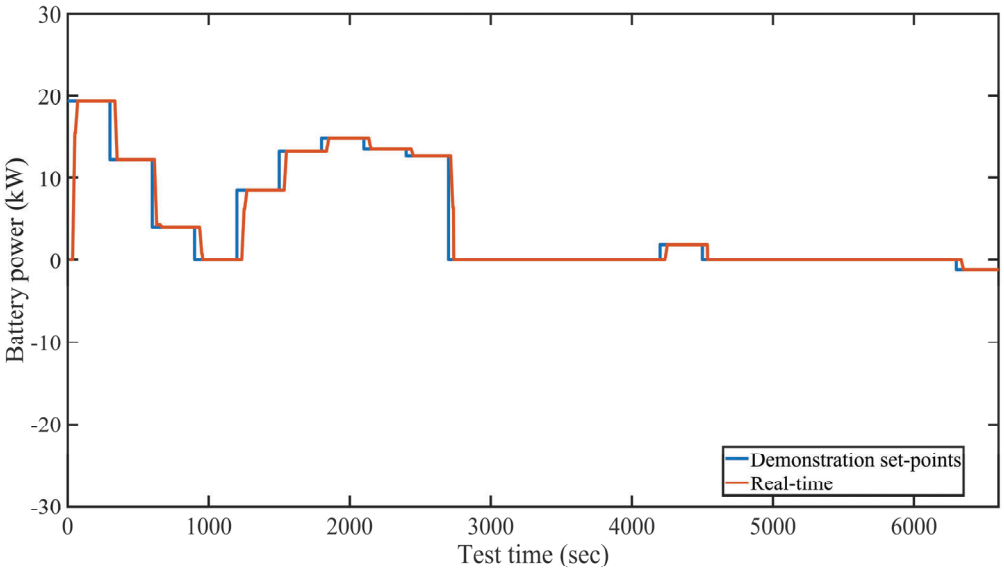

Figure 13 : The set-points and real-time measurements of the BESS in Brf Viva (Test D1.A on February 24, 2020).

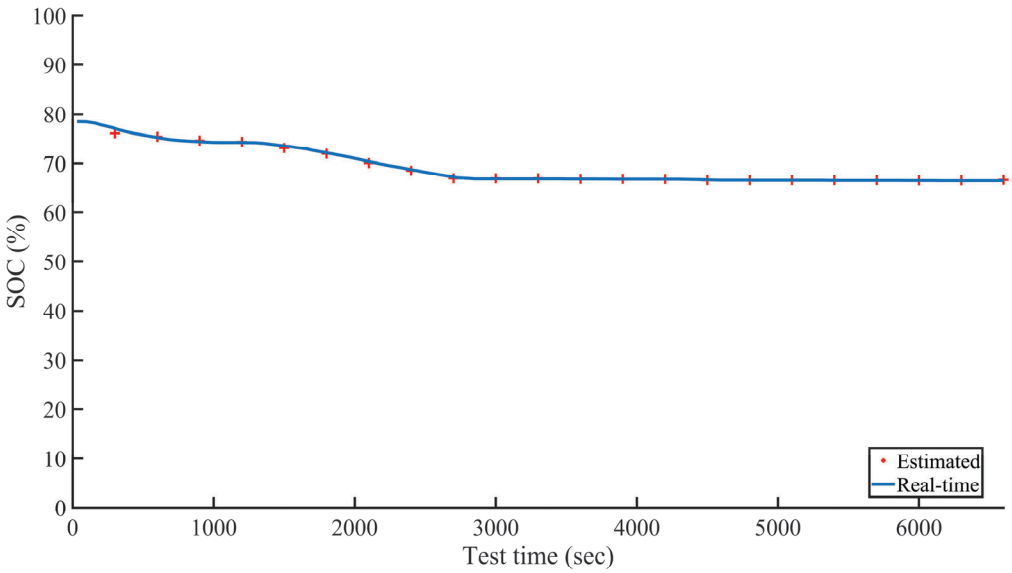

Figure 14 : The estimated SOC during the demonstration and the real-time value of SOC (updated per minute) of Brf Viva BESS (Test D1.A on February 24).

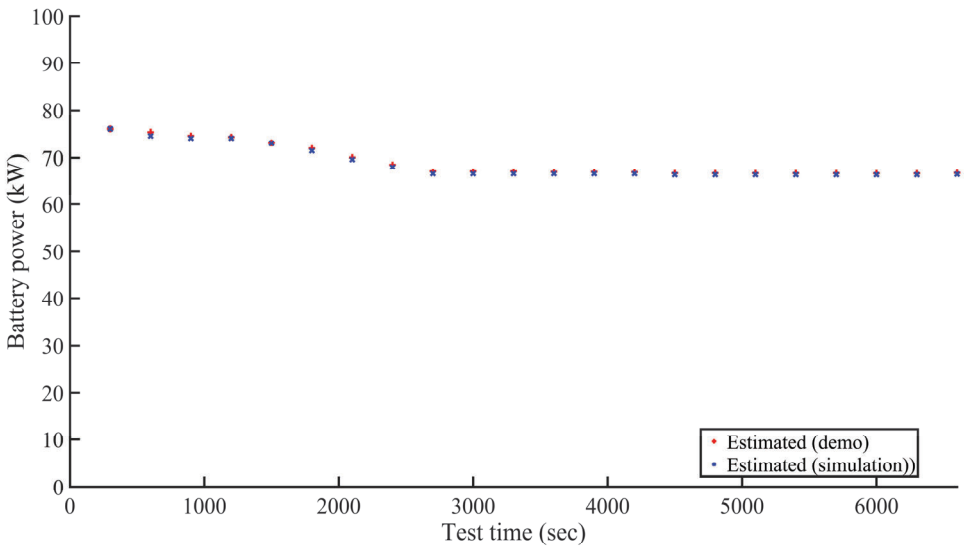

Figure 15 : The estimated SOC during the simulation and the real-site implementation (demonstration) of the rule-based algorithm (Test D1.A on February 24, 2020).

The estimation of the SOC using the ideal BESS model is almost completely accurate as Figure 14 shows. In addition, the estimated battery power set-points and SOC of simulation tests matched exactly the values from the demonstration. The same can be observed from the demonstration results of Test D1.B, which can be seen in Figure 16. The SOC values shown in Figure 16 correspond to constant discharging power-setpoints of 30 kW (updated per 5 minutes) dispatched according to the solution of Test D1.B. The update of the SOC measurement per 5 minutes gives again very good results. The SOC estimation during demonstration was slightly less accurate for Test D1.B than D1.A (see Figure 14 and Figure 16) due to higher discharge power rate in Test D1.B. When charging or discharging C-rate of the battery increases, the respective efficiency decreases [9].

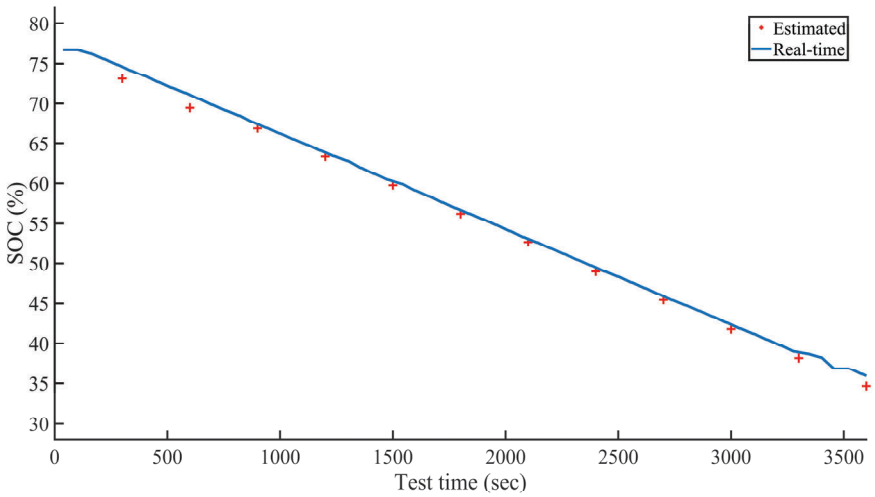

Figure 16 : The estimated SOC during the demonstration and the real-time value of SOC (updated per minute) of Brf Viva BESS (Test D1.B on February 25, 2020).

The accuracy of the ideal BESS model was also demonstrated with a 15-minute battery scheduling i.e., the battery power dispatch and the update of SOC online measurement was done per 15 minutes (Figure 17). For comparison, a demonstration of the same test (same load, PV, and price input as well as time resolution) using the NIDD-BESS model can be seen in Figure 18. The accuracy of the SOC estimation with both the ideal BESS model and the NIDD-BESS model is very good for close to real-time battery scheduling (5-15 min time resolution).

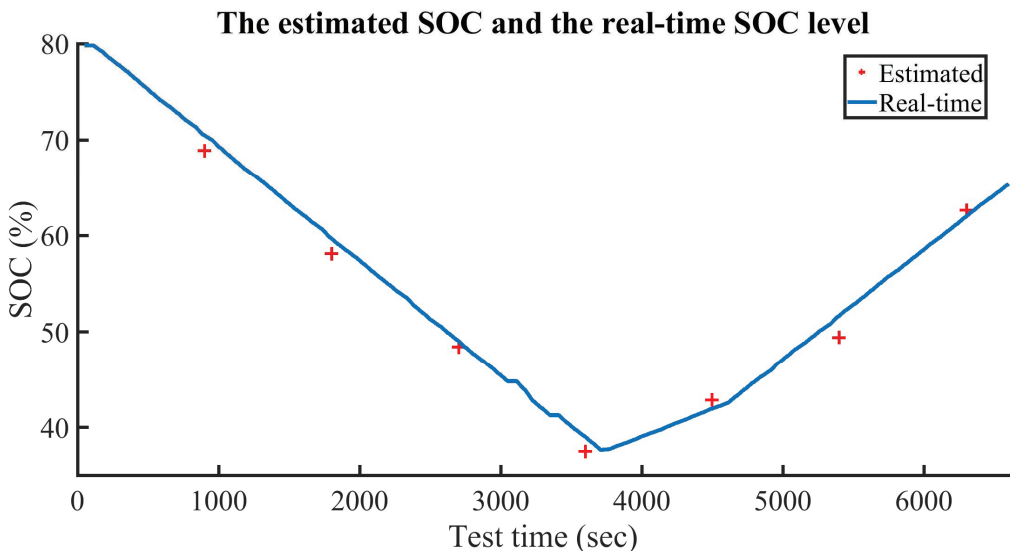

Figure 17 : A demonstration of power dispatch were the ideal BESS is used. The SOC measurement (input to the algorithm) is updated per 15 min.

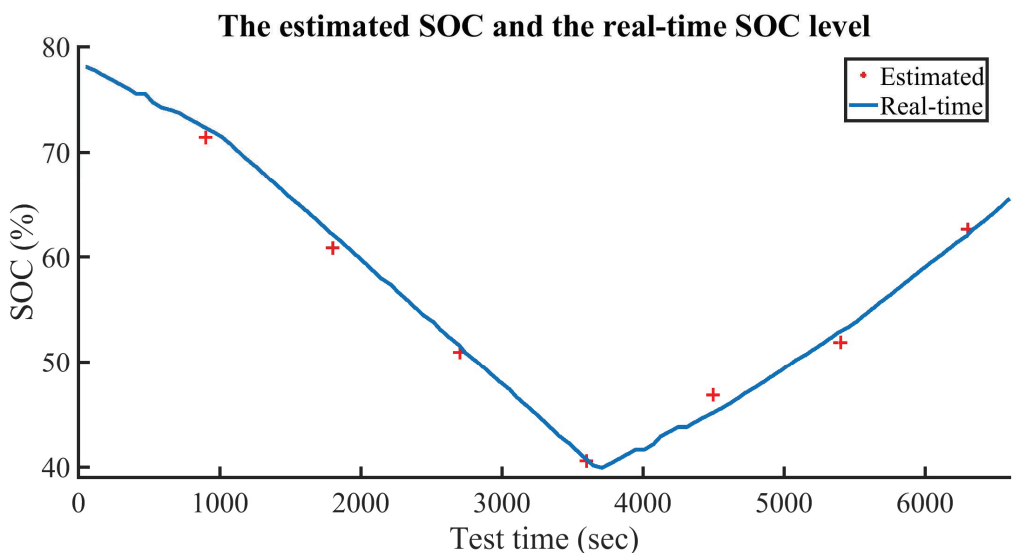

Figure 18 : A demonstration of power dispatch were the NIDD-BESS is used. The SOC measurement (input to the algorithm) is updated per 15 min.

The battery scheduling implemented by Tests D1.B-D1.D also considered the spot market price and the same input (the day-ahead spot market electricity price, which is given in Table 2) was used in all cases. The results from the demonstration of Test D1.C can be seen in Figure 19-Figure 22, while the results from Test D1.D can be seen in Figure 23-Figure 26.

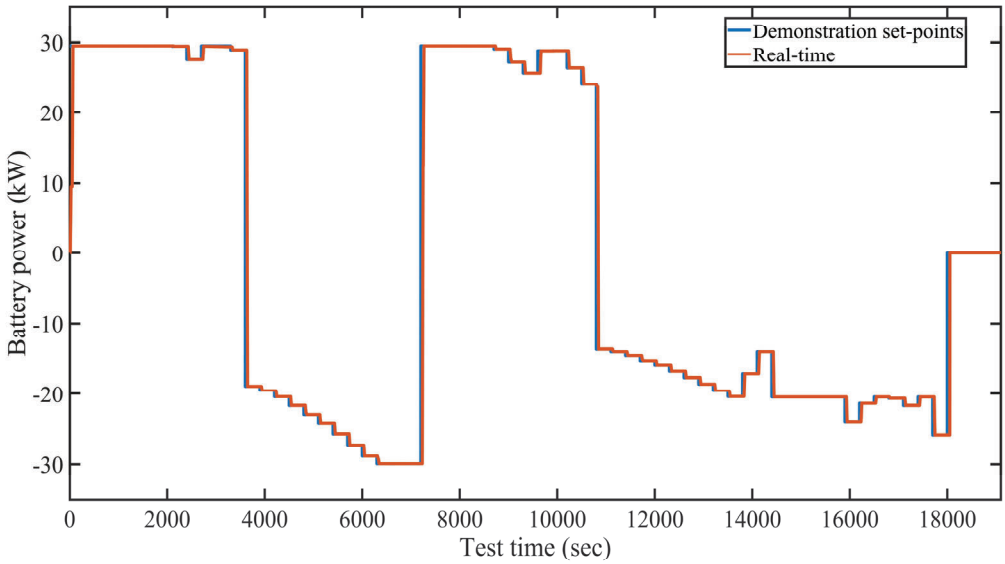

Figure 19: The set-points and real-time measurements of the BESS in Brf Viva (Test D1.C on February 26, 2020).

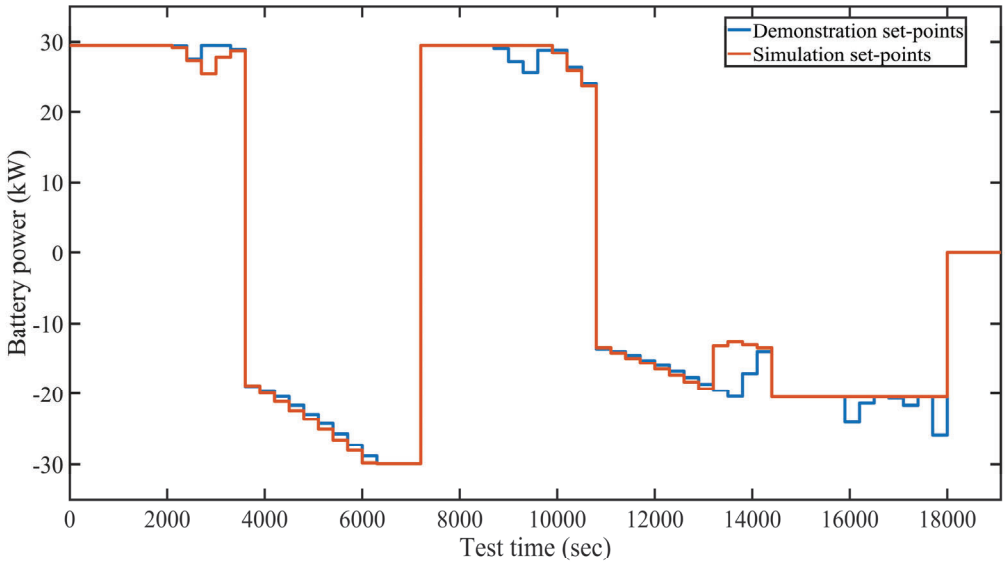

Figure 20 : The battery power set-points of simulation and demonstration test in Brf Viva (Test D1.C on February 26, 2020).

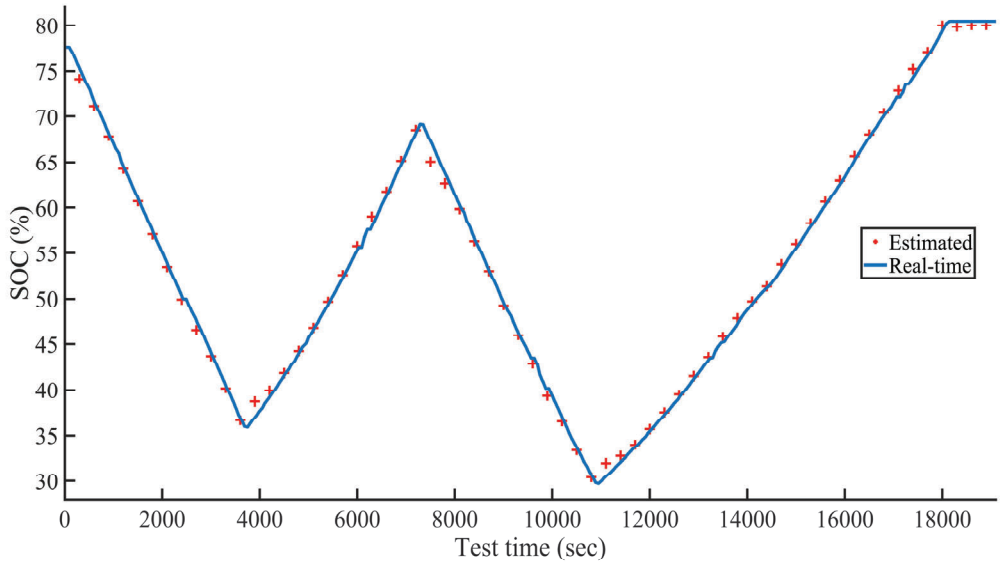

Figure 21 : The estimated SOC during the demonstration and the real-time value of SOC (updated per minute) of Brf Viva BESS (Test D1.C on February 26, 2020).

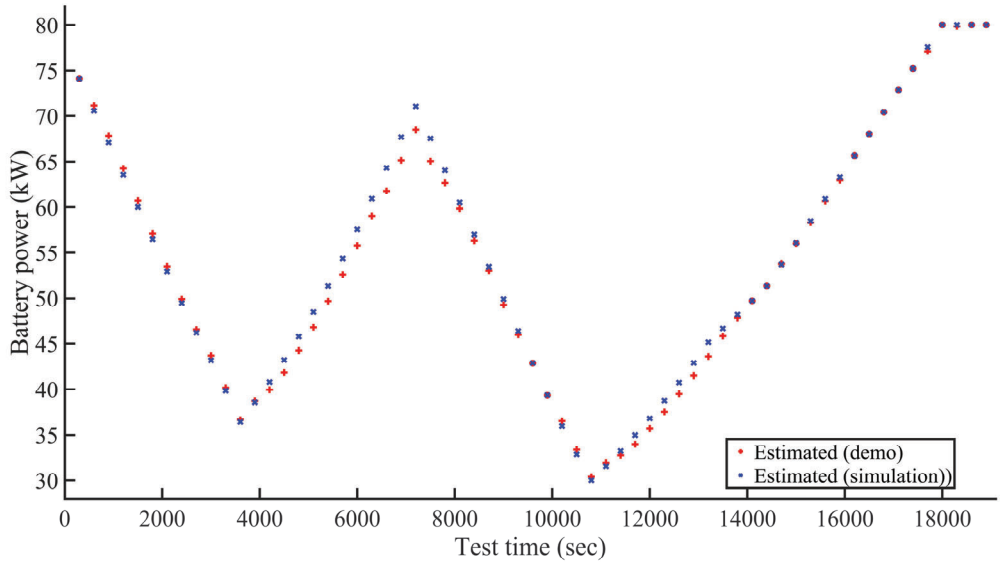

Figure 22 : The estimated SOC during the simulation and the real-site implementation (demonstration) of the energy cost minimization algorithm in Brf Viva (Test D1.C on February 26, 2020).

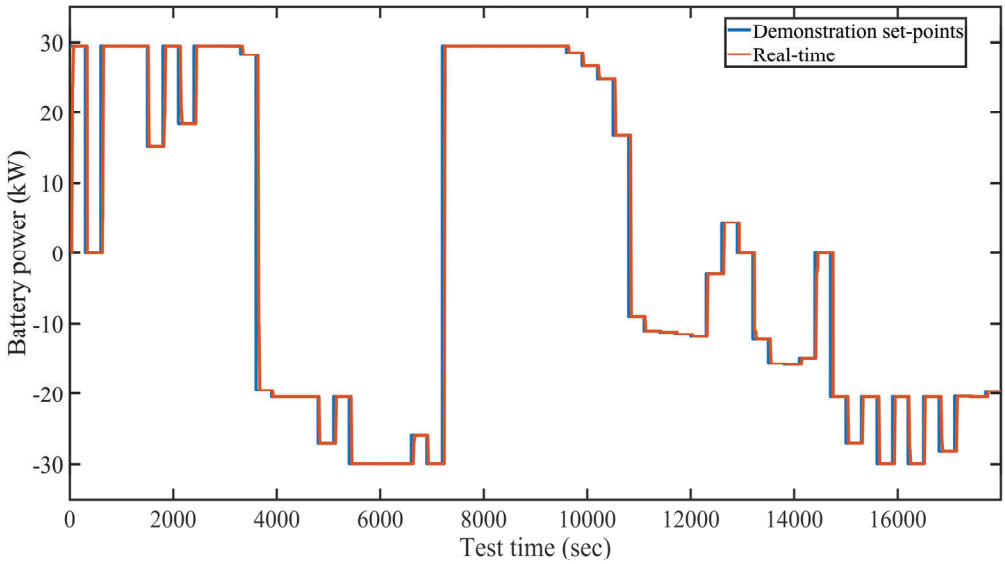

Figure 23 : The battery power set-points of simulation and demonstration test in Brf Viva (Test D1.D on February 27, 2020).

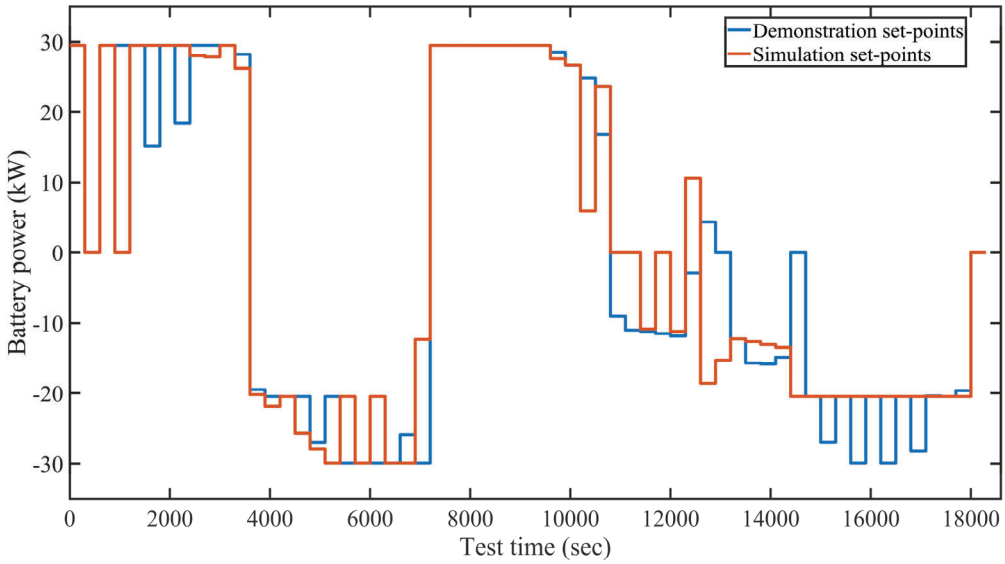

Figure 24 : The battery power set-points of simulation and demonstration test in Brf Viva (Test D1.D on February 27, 2020).

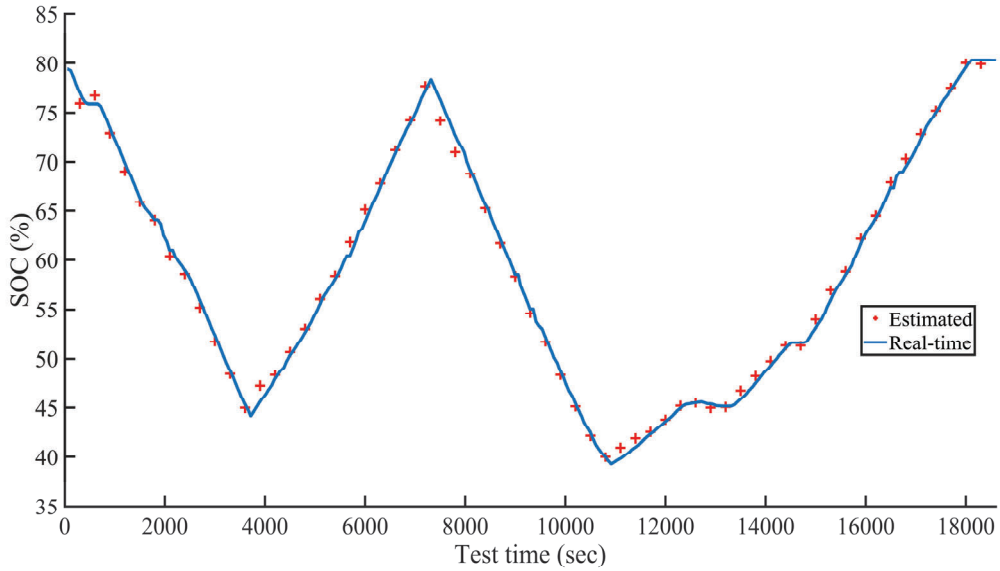

Figure 25 : The estimated SOC during the demonstration and the real-time value of SOC (updated per minute) of Brf Viva BESS (Test D1.D on February 27, 2020).

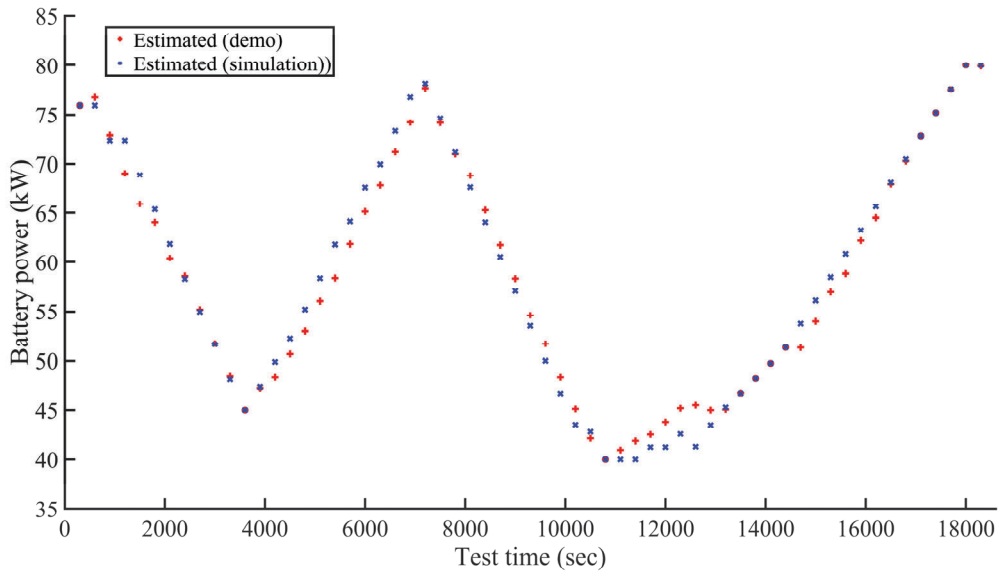

Figure 26 : The estimated SOC during the simulation and the real-site implementation (demonstration) of the energy cost minimization algorithm in Brf Viva (Test D1.D on February 27, 2020).

5.1.4 Estimated and actual cost

Table 5 presents the comparison of the cost that the battery power set-points yield during demonstration and the expected cost that the battery power set-points of the simulation would yield. Similarly, Table 6 presents the comparison between the expected and the actual peak demand. In both cases, the

load and PV generation profiles are considered as inputs to the model with precise forecasted values and the forecast errors are not considered. The differences in the expected and actual cost as well as the expected and actual peak power show the effect of SOC estimation and delivered battery power. The cost is given for the time period each demonstration lasted, so differences between the Test D1.A with the Test D1.C-D should not be compared. Tests D1.C-D were run for the same time period (6 hours) and the costs are similar as the dispatch of the batteries is also very similar for this time period.

Table 5 : Comparison between simulation (expected cost) and demonstration (actual cost) for DemoCase1

Test #	Expected cost (simulation)	Actual cost (demonstration)	Deviation (%)
D1.B	14.6 SEK	14.6 SEK	0 %
D1.C	73.4 SEK	73.6 SEK	+ 0.27 %
D1.D	74.1 SEK	73.9 SEK	- 0.27 %

Table 6 : Comparison between simulation (expected peak) and demonstration (actual peak) for DemoCase1

Test #	Expected peak (simulation)	Actual peak (demonstration)	Deviation (%)
D1.B	70.5 kW	70.5 kW	0
D1.C	105.4 kW	105.4 kW	+ 0 %
D1.D	106.7 kW	106 kW	- 0.66 %

5.2 DemoCase1 in HSB LL

5.2.1 Demonstration results of preliminary Tests D1.A-D1.B

Figure 27 shows the battery response in HSB LL during a preliminary demonstration of Test D1.A, while Figure 28 shows the battery response during a preliminary demonstration of Test D1.C. In both cases, the time-scale of battery control and feedback of SOC measurement is 5 minutes. These preliminary tests showed good response of the battery to the dispatched set-points and the average communication delay (from the time that the set-point is dispatched until the time that the battery responds with the desired power input/output) was about 30 sec.

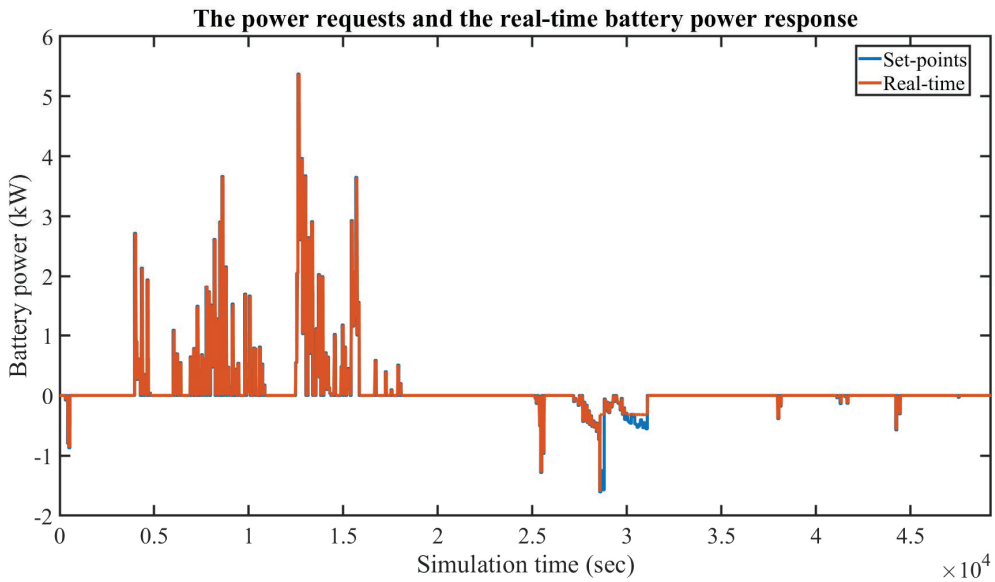

Figure 27 : The set-points and real-time measurements of the battery power in HSB LL (Test D1.A on 31 January, 2020).

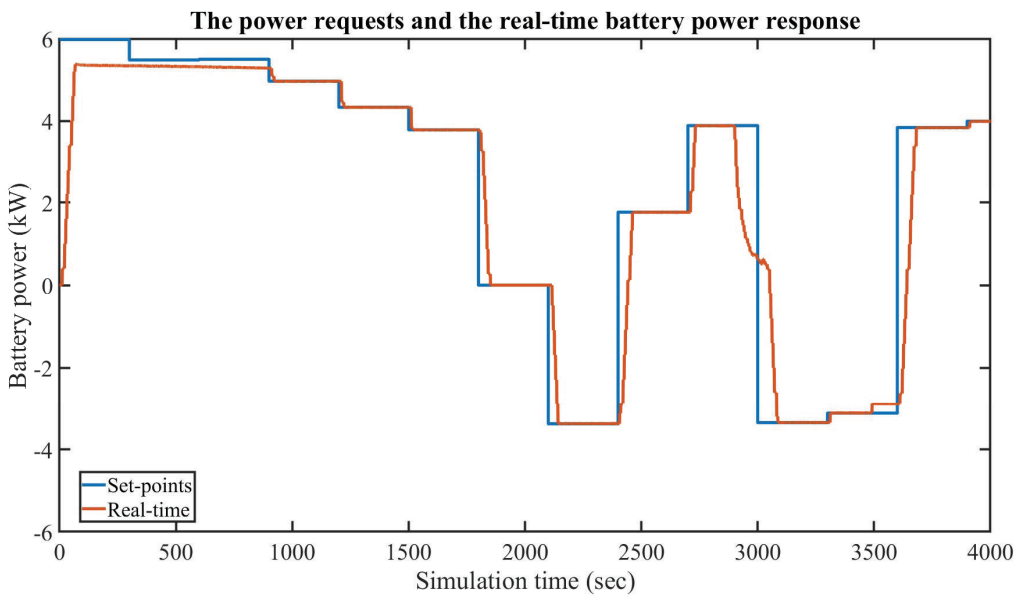

Figure 28 : The set-points and real-time measurements of the battery power in HSB LL (Test D1.C on 23 January, 2020).

5.2.2 Demonstration results for Tests D1.B-C

The energy cost minimization algorithm with the ideal BESS model (Test D1.B of DemoCase1) and with the NIDD BESS model (Test D1.C of DemoCase1) was demonstrated in HSB LL for 24 hours with 15 min and 1 h time-scale. In all the demonstrations, the same load and PV data (perfect forecast was assumed) as well as electricity price data were used as input. The difference between the tests were related to the use of BESS model, the time-scale (time-discretization step) and the maximum charging power limit. For

the ideal BESS model, the average charging and discharging efficiency from the experimental measurements were used, which was 92% for charging efficiency and 98% for discharging efficiency. The demonstration of Test D1.B with a 15 min time-scale and an upper limit on charging power of 3 kW is shown in Figure 29-Figure 32.

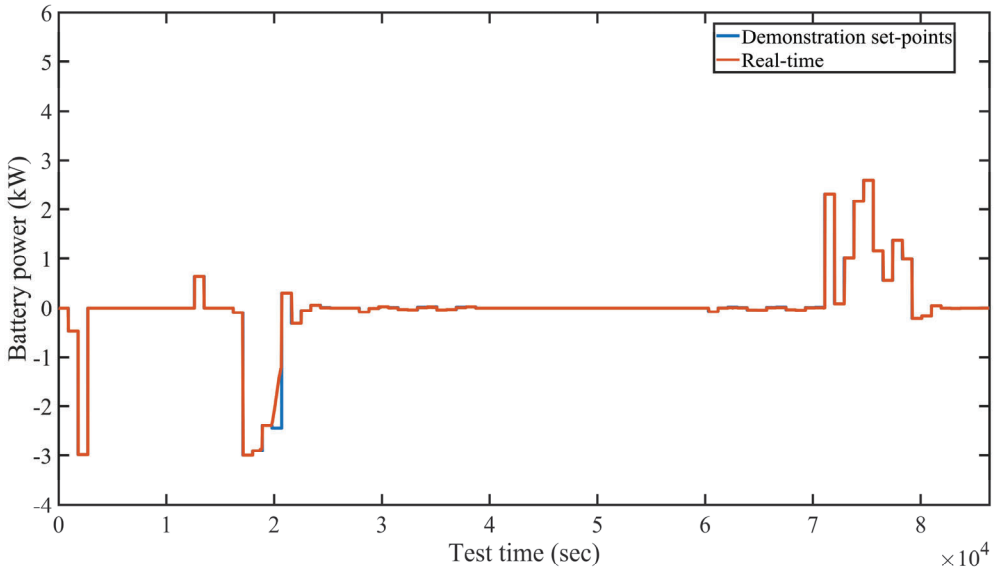

Figure 29 : The set-points and real-time measurements of the BESS in HSB LL (Test D1.B on February 29-March 1, 2020).

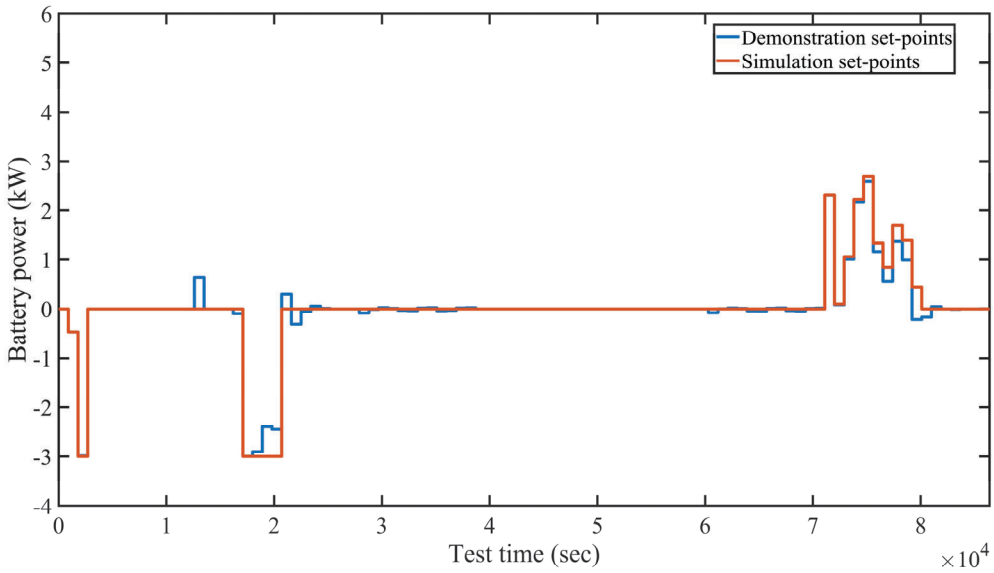

Figure 30 : The battery power set-points of simulation and demonstration test in HSB LL (Test D1.B on February 29-March 1, 2020).

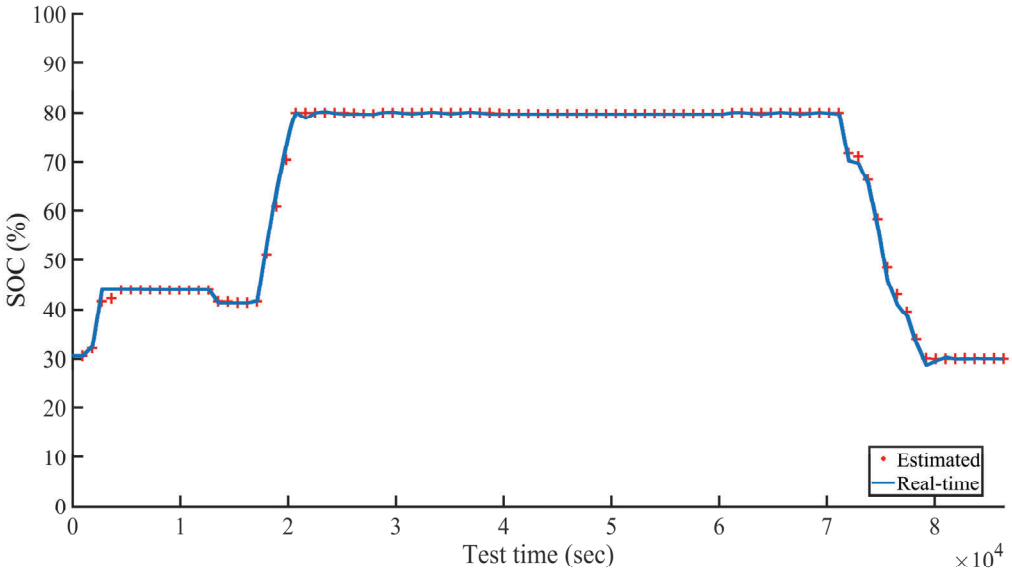

Figure 31 : The estimated SOC during the demonstration and the real-time value of SOC (updated per 5 sec) of HSB LL BESS (Test D1.B on February 29-March 1, 2020).

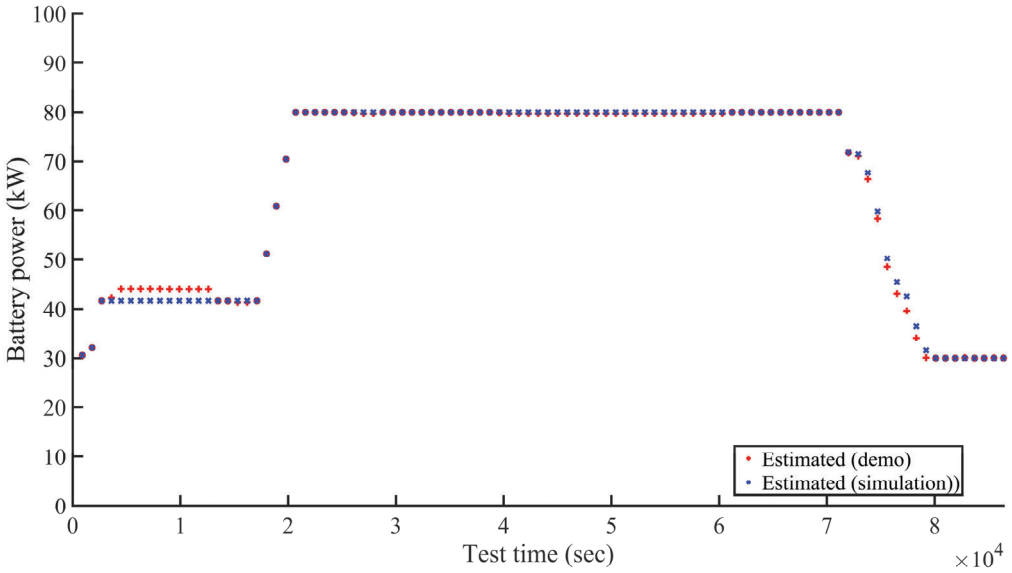

Figure 32 : The estimated SOC during the simulation and the real-site implementation (demonstration) of the rule-based algorithm (HSB LL, Test D1.B on February 29-March 1, 2020).

The demonstration of Test D1.B with a time-scale of 1 hour and an upper limit on charging power of 3 kW is shown in Figure 33 and Figure 34. Here, there is a noticeable difference between the set-points and the dispatched power, when the algorithm send a zero output command after the battery had been charging. This can be explained by the fact that the upper SOC limit set by the BIMG-EMS is violated at the end of the previous (hourly) time-step. So, although a zero battery power set-point was to be implemented according to the algortihm's decision, the BIMG-EMS overrules this and sends a low

discharging command to reduce the high SOC. It can be seen that without frequent feedback of the SOC measurement, the deviation of the estimated SOC from the SOC measurement provided by the converter can be significant (see Figure 34). The ideal BESS model is thus regarded as not appropriate for hourly battery scheduling in HSB LL (neither for online application nor for studies regarding operation and planning of the BIMG).

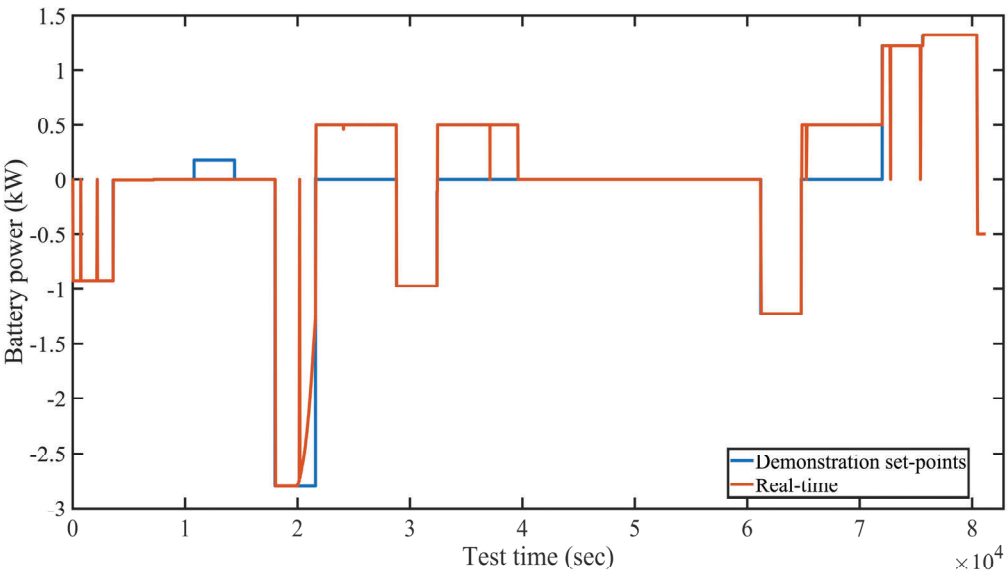

Figure 33 : The set-points and real-time measurements of the BESS in HSB LL (Test D1.B on 1-2 March, 2020).

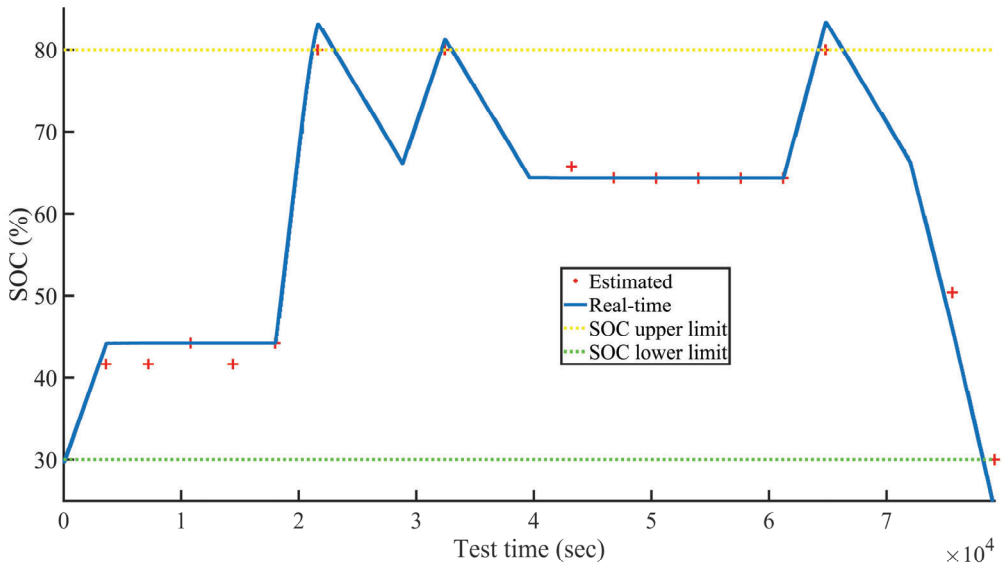

Figure 34 : The estimated SOC and the real-time value of SOC (updated per 5 sec) of the BESS in HSB LL (Test D1.B on 1-2 March, 2020).

Stationary application of batteries, in contrast with electric vehicle applications, are high-energy based and operate in power levels, which are lower than their maximum capability. This means that the rated

power can be delivered unless the SOC is too low or too high, something which could trigger the current limiter function of the battery converter. The current limiter measures the storage voltage, is triggered by high/low thresholds and reduces battery current to zero at the end of charge/discharge voltage limits. It is the BMS that sets the end of charge/discharge voltage limits, which means that the actual 0 or 100% SOC of the installed battery is never reached during its operation, even if the battery operator applies no further SOC limits. This is done to avoid too high stress and protect the battery. In the battery operating region that is allowed by the BMS, the power output is more predictable due to relatively stable voltage values.

However, if the state-of-health (SOH) of the battery has deteriorated e.g., if a number of battery cells has degraded significantly, non-linear behaviour of the battery could be observed within the normal operating region of SOC i.e., the rated power might not always be delivered. The tests both in Brf Viva and in HSB LL were applied for SOC values that could not trigger the current limiter.

DemoCase1 in Brf Viva proved that the rated power was delivered, as the results in Section 5.1 show. In the HSB LL demonstrations, however, non-linear battery power charging was observed. A demonstration of Test D1.B with higher allowable charging C-rates by the energy cost minimization algorithm at the HSB LL battery showed that the ideal BESS could not always deliver the rated power. The results from Test D1.B with maximum charging power at 4 kW and a 15 min time-scale can be seen in Figure 35-Figure 38.

As can be seen, there are violations in the SOC limits; however, they are small, since the SOC is updated per 15 min and such violations are less likely to happen with the 5 min time-scale, as other tests have shown. The non-linear battery power behaviour can be observed in Figure 35. Although, previous demonstration tests in HSB LL showed that the battery power dispatch would match exactly the battery power request (with a small time-delay due to the communication protocols), this case shows that the charging request cannot be met. The SOH of the battery in HSB LL reduces even further the accuracy of the ideal model, which assumes that the limits on maximum power are constant.

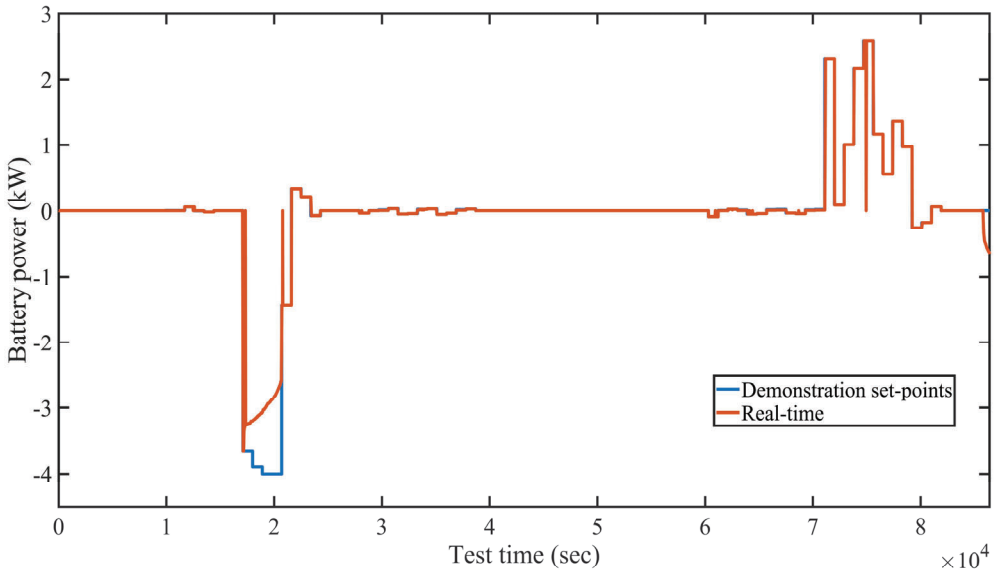

Figure 35 : The set-points and real-time measurements of the BESS in HSB LL (Test D1.B on 3-4 March, 2020).

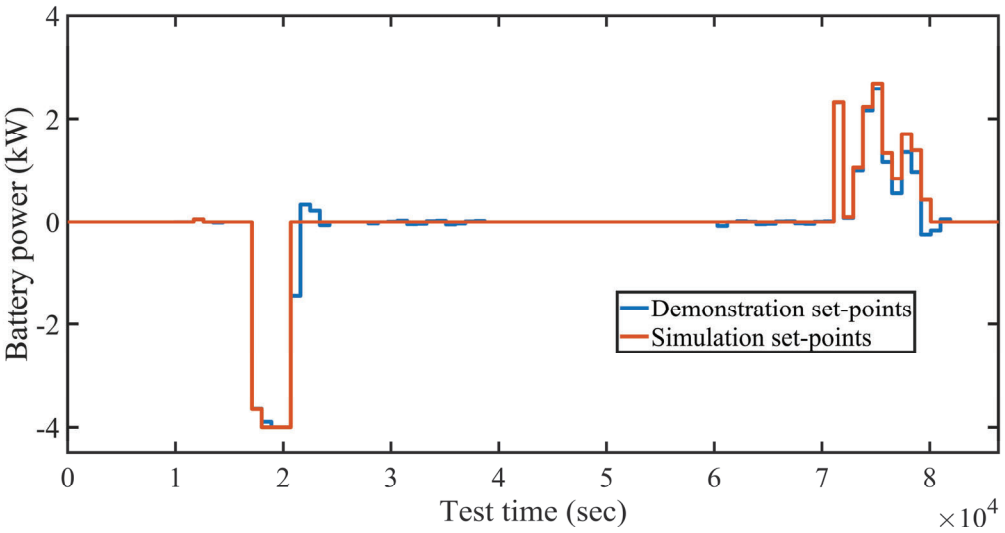

Figure 36 : The battery power set-points of simulation and demonstration test in HSB LL (Test D1.B on 3-4 March, 2020).

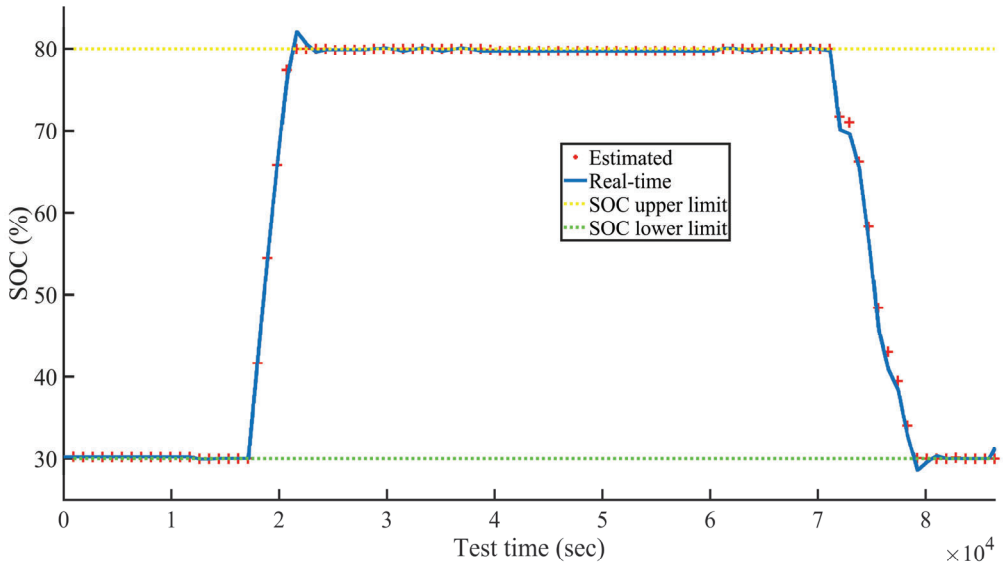

Figure 37 : The estimated SOC and the real-time value of SOC (updated per 5 sec) of the BESS in HSB LL (Test D1.B on 3-4 March, 2020).

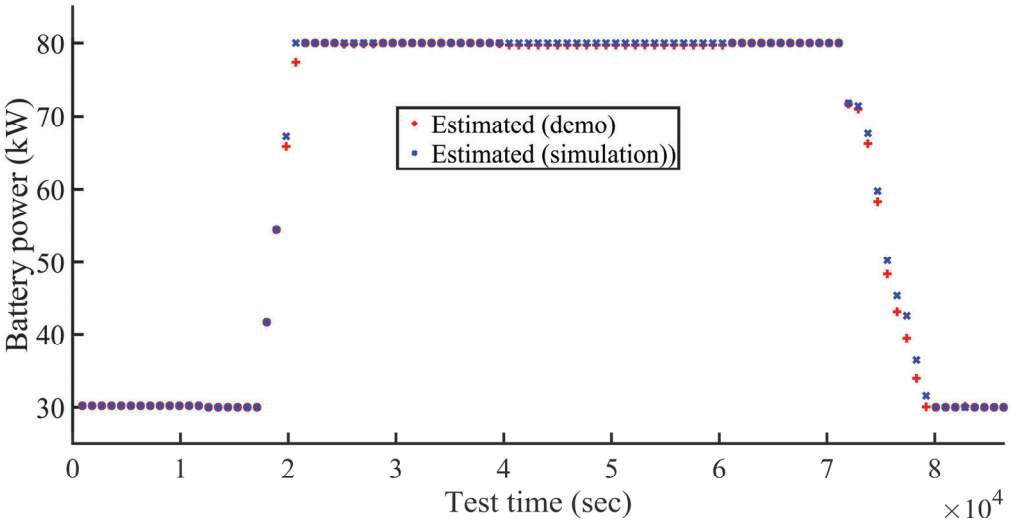

Figure 38 : The estimated SOC during the simulation and the real-site implementation (demonstration) of the rule-based algorithm (Test D1.B on 3-4 March, 2020).

Figure 39 shows the battery voltage during a discharging test of the battery at the HSB LL at rated power (6 kW). The battery voltage is noticeably decreased at 30%. Unstable battery voltage in normal operating SOC region will trigger the current limiter and requested power will be reduced.

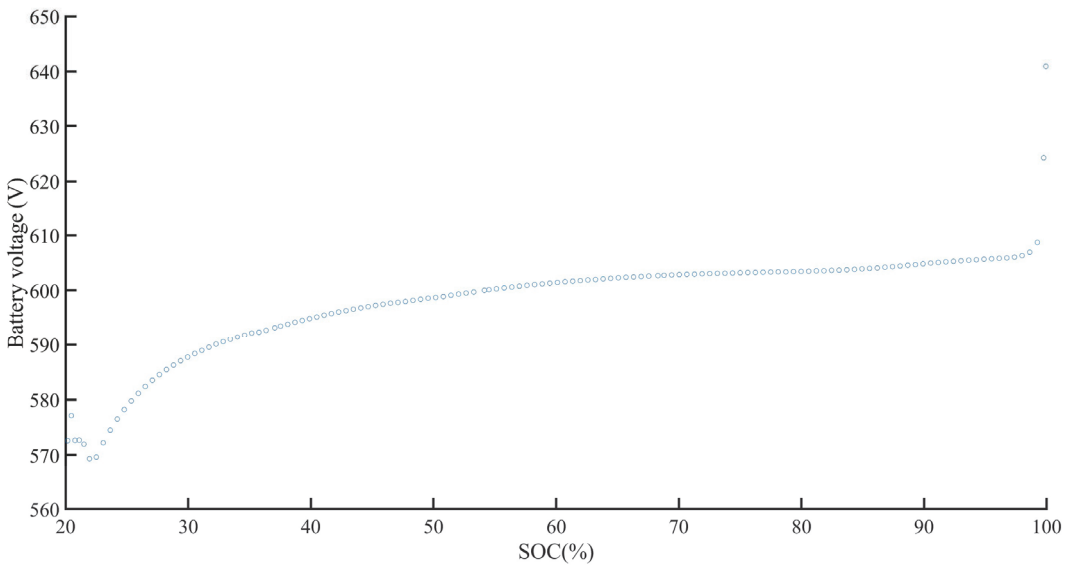

Figure 39 : Battery voltage curve as a function of SOC during a discharging test with the HSB LL battery with rated power (6 kW).

The results from Test D1.C with maximum charging power at 4 kW and a 15 min time-scale can be seen in Figure 40-Figure 43. Comparing Figure 40 with Figure 35 one can notice that the response to the battery power set-points is improved in Test D1.C.

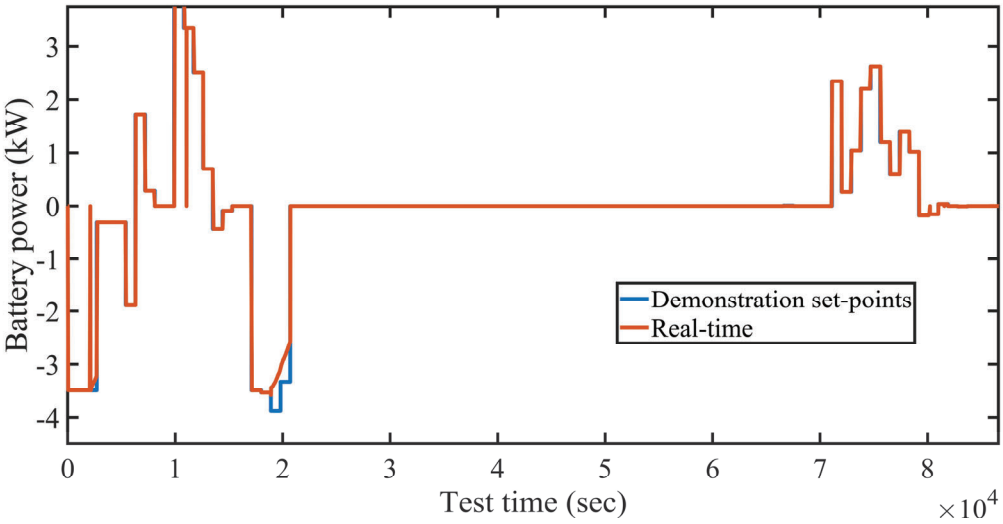

Figure 40 : The set-points and real-time measurements of the BESS in HSB LL (Test D1.C on 15-16 March, 2020).

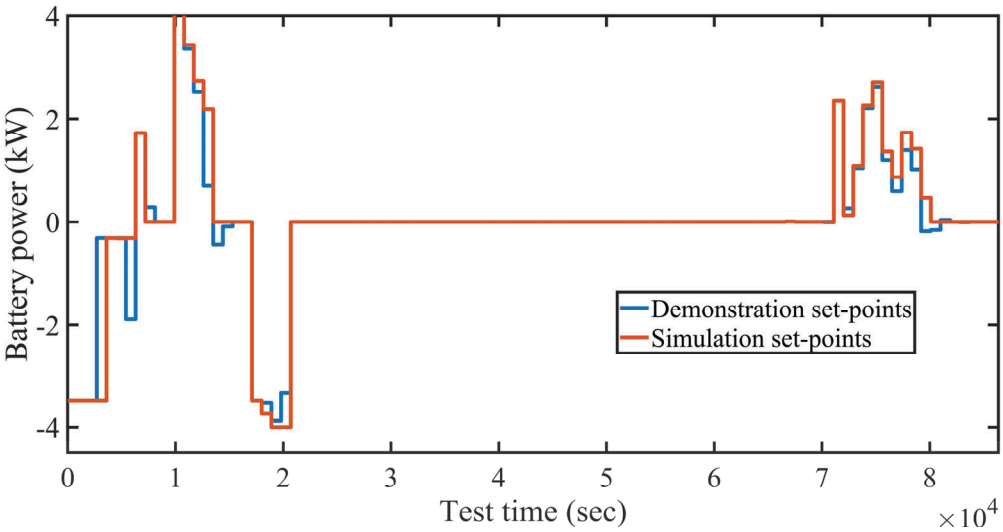

Figure 41 : The battery power set-points of simulation and demonstration test in HSB LL (Test D1.C on 15-16 March, 2020).

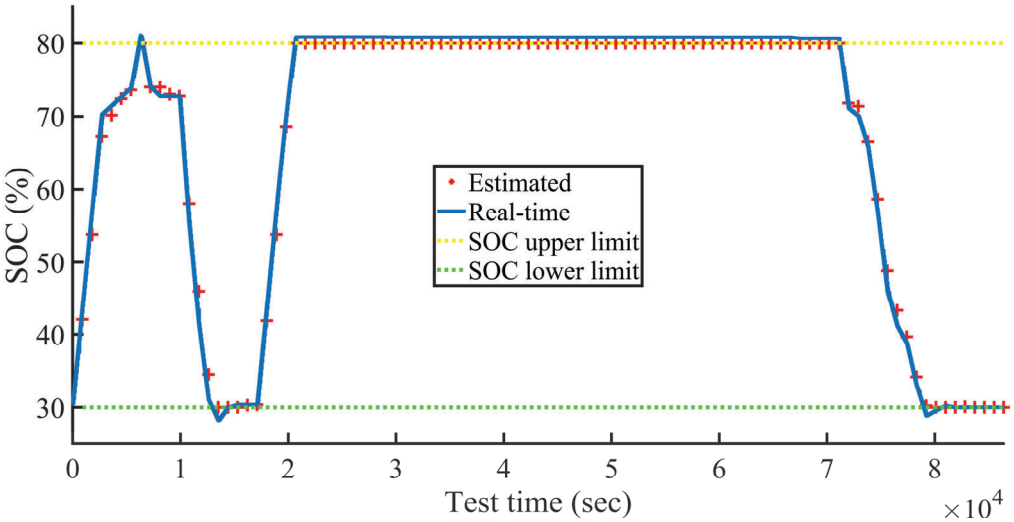

Figure 42 : The estimated SOC and the real-time value of SOC (updated per 5 sec) of the BESS in HSB LL (Test D1.C on 15-16 March, 2020).

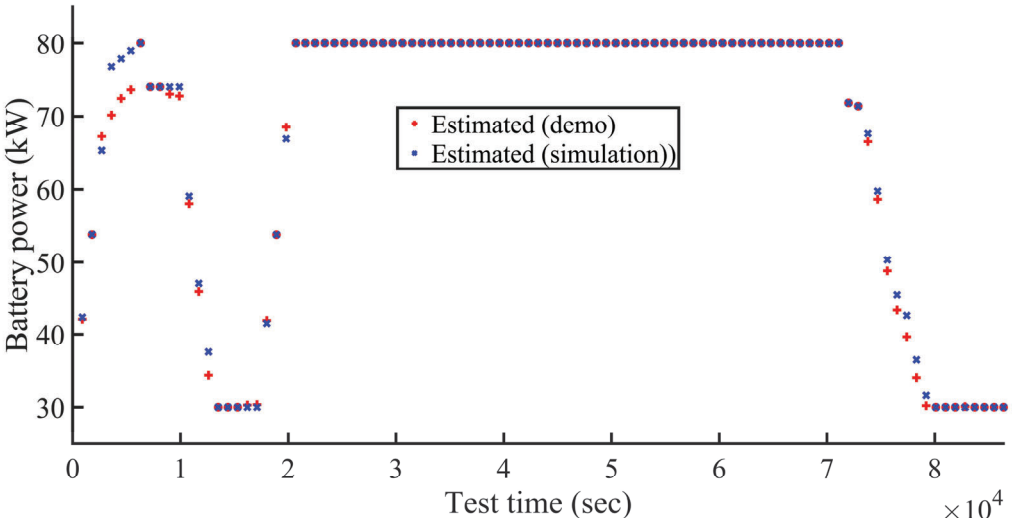

Figure 43 : The estimated SOC during the simulation and the real-site implementation (demonstration) of the rule-based algorithm (Test D1.C on 15-16 March, 2020).

5.2.3 Estimated and actual cost

Table 7 presents the comparison of the daily cost that the battery power set-points yield during the demonstration and the expected cost that the battery power set-points of the simulation would yield. Similarly, Table 8 presents a comparison between the expected and the actual cost. Both the simulation and the demonstration of Test D1.B and Test D1.C assume the same input, i.e., load, PV generation, electricity price, and initial SOC. In the demonstration, the actual SOC and battery power measurements (provided by the converter) are used instead of the estimated values, which are the simulation results, to calculate the actual cost and peak power. The differences in the expected and actual cost as well as the expected and actual peak power reflect the accuracy of each model with respect to SOC and battery power estimation.

Table 7 : Comparison between simulation (expected cost) and demonstration (actual cost) for DemoCase1

Test #	Expected cost (simulation)	Actual cost (demonstration)	Deviation (%)
D1.B	71.6 SEK	72.6 SEK	1.4 %
D1.C	71.5 SEK	72.6 SEK	1.5 %

Table 8 : Comparison between simulation (expected peak) and demonstration (actual peak) for DemoCase1

Test #	Expected peak (simulation)	Actual peak (demonstration)	Deviation (%)
D1.B	16.8 kW	17.5 kW	4.2 %
D1.C	16.8 kW	17.5 kW	4.2 %

Even though the metrics of Test D1.B and Test D1.C (Table 7 and Table 8) for this specific 24-h demonstration were identical, the battery scheduling is very different. In Test D1.C, the total energy mismatch was 0.51 kWh, whereas in Test D1.B the energy mismatch was 1 kWh i.e., 96% increased. This proves the benefit of using the NIDD-BESS model, as it is more accurate.

5.3 DemoCase2

5.3.1 DSO and BIMGs flexibility coordination platform

In this section, the coordination platform for trading flexibility ("Flexibility market" in Figure 7) is explained. The coordination platform is activated in case of a need for flexibility from the DSO. In this demo case, overloading of a transformer is assumed as the cause for the flexibility need.

When the coordination platform is activated, it receives bid curves from flexibility providers and flexibility buyers. The bid curves include the different levels of flexibility in the form of power and the corresponding prices per each unit of power. Afterwards, the bid curves are merged and sorted based on the prices to form the demand and supply curves. By intersecting the supply and demand curve, the cleared price and power are sent back to the BIMGs.

5.3.1.1 The supply bids

The provided bids from the two demo sites, i.e., Brf Viva and HSB LL, and the merged supply bids are presented in Figure 44. The bids are different because the NIDD-BESS model represents more accurately the actual battery behavior.

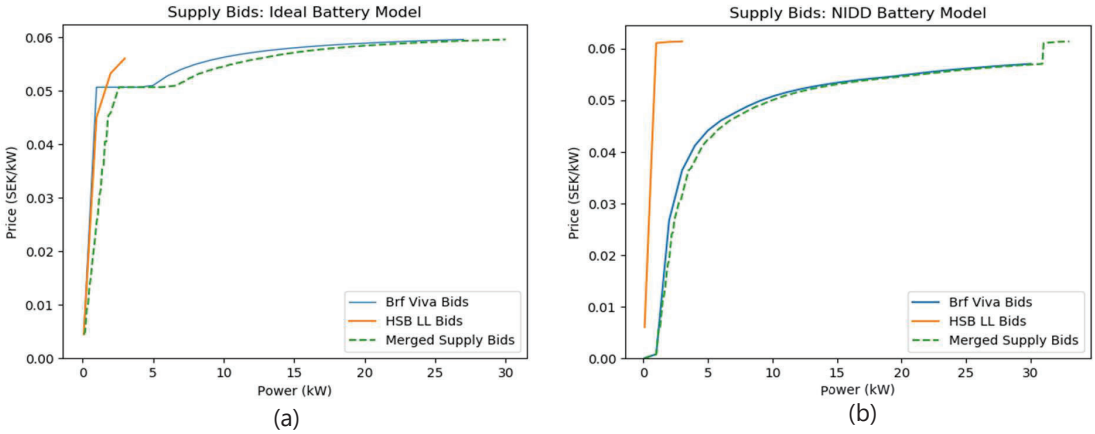

Figure 44: Supply bids of the two BIMGs using (a) the ideal BESS model and (b) the NIDD-BESS model

First, the two BIMGs solve the energy cost minimization algorithm with a time-discretization step of 1 hour to obtain the optimal battery power dispatch for the next hour. Then, they calculate the flexibility amounts they can provide for the next hour as well as the price per MW that they should receive for this flexibility. The feasibility of the flexibility amounts is dependent on the energy storage capacity for each building, the energy storage levels at the time of the flexibility request, the charging and discharging efficiency (denoted by η_{ch} and η_{dis}, respectively) of each energy storage system, and the maximum and minimum state-of-charge-limits that each building operator has decided for the BESS operation.

The BESS initial conditions and characteristics of the two BIMGs before the flexibility requests are given in Table 9.

Table 9 : The initial conditions and characteristics of DemoCase2 (considering ideal BESS)

	HSB LL	**Brf Viva**
Rated storage capacity	7.2 kWh	70.5 kWh
Initial SOC	68.11 %	67.06 %
$\boldsymbol{\eta_{ch}/\eta_{dis}}$	0.92/0.98	0.97/0.97
$\boldsymbol{SOC_{min}/SOC_{max}}$	30%/80%	30%/80%

The cost per MW for each flexibility amount is dependent on the price difference between the initially optimal cost (initial solution of the energy cost minimization problem) and the optimal cost considering the dispatch of the cleared flexibility amount. This means that the two BIMGs solve the energy cost minimization algorithm for each scenario of dispatched flexibility to provide their supply bids to the DSO.

5.3.1.2 The demand bid

To calculate the demand curve, loss of life of the transformer is calculated based on IEEE C5791-2011 Clause 7 [13]. Afterwards, in an iterative procedure, the loss of life is re-calculated by reducing the over-loading. The benefit from the flexibility is calculated by the reduction in the loss of life which is caused by the purchasing flexibility. The DSO's demand bids are presented in Figure 45.

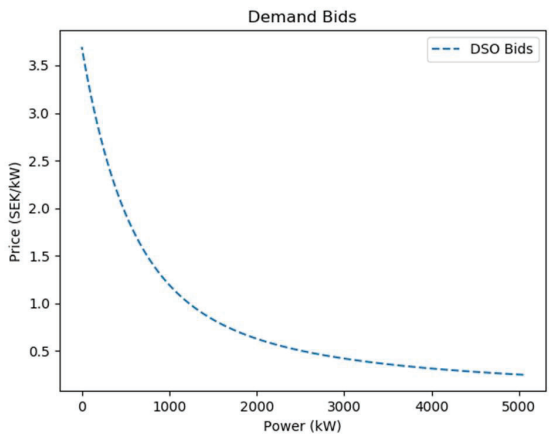

Figure 45 DSO demand bids

5.3.1.3 Clearance in the flexibility coordination platform

The supply and demand curves are presented in Figure 46 for the ideal battery model. As can be seen, the available flexibility is not enough to support all the DSO's needs. However, it is assumed that DSO would yet be interested in purchasing the maximum available flexibility. In a real-life scenario, the flexibility request would anyway be sent to more BIMGs. Since the supply and demand curves do not have any intersection, the negotiated price was assumed to be the average of the supply and demand price at the maximum provided power by BIMGs.

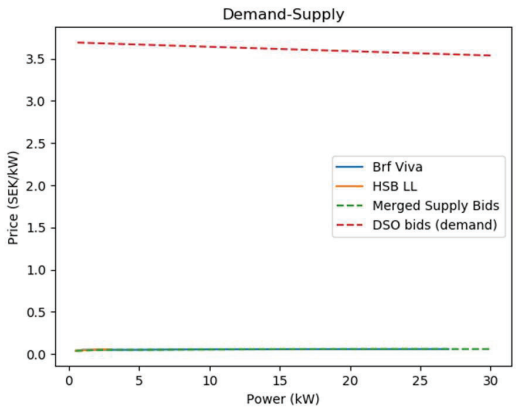

Figure 46 Flexibility supply and demand curves for ideal battery model

5.3.2 Demonstration of the flexibility dispatch

After the market clearing, the DSO sent to the BIMGs the flexibility requests and the BIMGs solved again their energy cost minimization algorithms considering these requests in order to finalize their optimal battery scheduling. The results can be seen in Figure 47-Figure 50, where it is proved that the BIMGs can assist the DSO in providing battery flexibility, as the dispatched battery power matches exactly the request with only a small fluctuation in the delivered power by HSB LL (Figure 48). Without frequent feedback of the SOC measurement as in DemoCase1, where demonstrated time-scale of the battery scheduling was 5-15 min, the SOC measurement at the end of the first hour, when flexibility is dispatched, deviates from the estimated SOC (Figure 49-Figure 50). Specifically, it is underestimated by 5.8 % in Brf

Viva and it is overestimated by 11.4 % in HSB LL. It is therefore clear that the use of the ideal BESS model with hourly update of battery set-points serves the DSO by providing the cleared flexibility amount, as results prove that cleared power is delivered. It is, however, less suitable for building operators because the deviation in estimated SOC is significant and could lead to deviations in the expected cost.

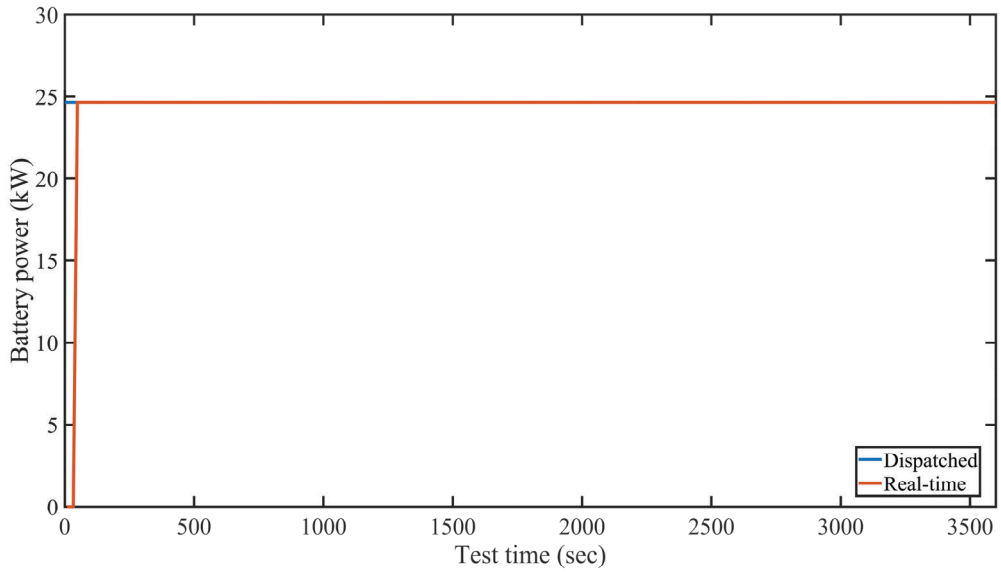

Figure 47 : The dispatched battery power of BrfViva BESS in DemoCase2 after the cleared flexibility amount.

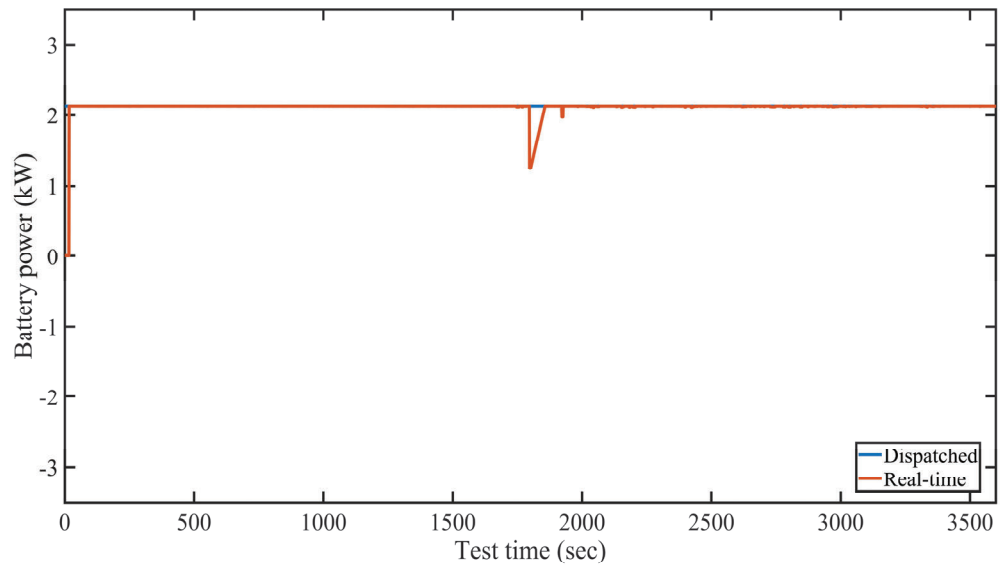

Figure 48 : The dispatched battery power of HSBLL BESS in DemoCase2 after the cleared flexibility amount.

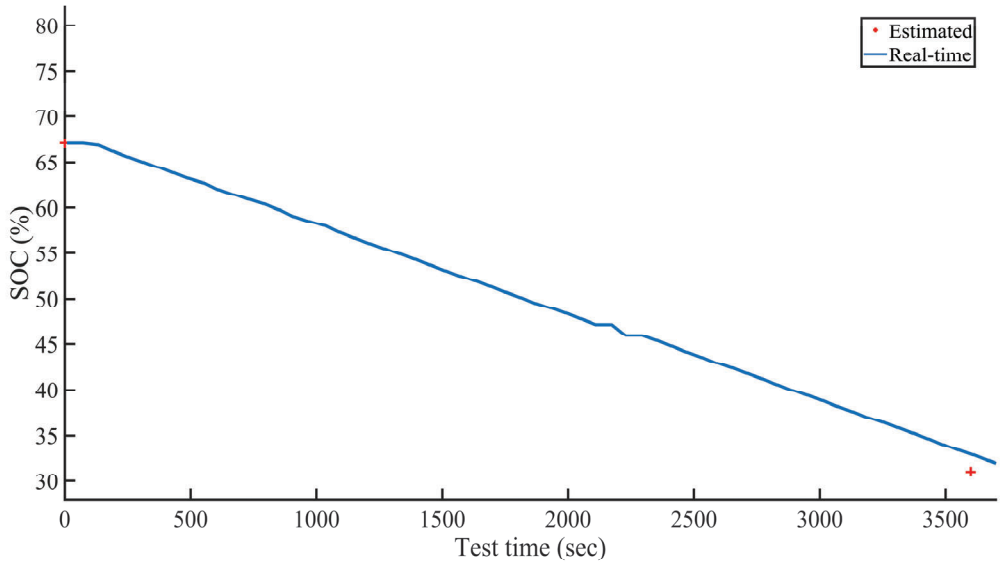

Figure 49 : The estimated SOC and the real-time value of SOC (updated per minute) of Brf Viva BESS (DemoCase2).

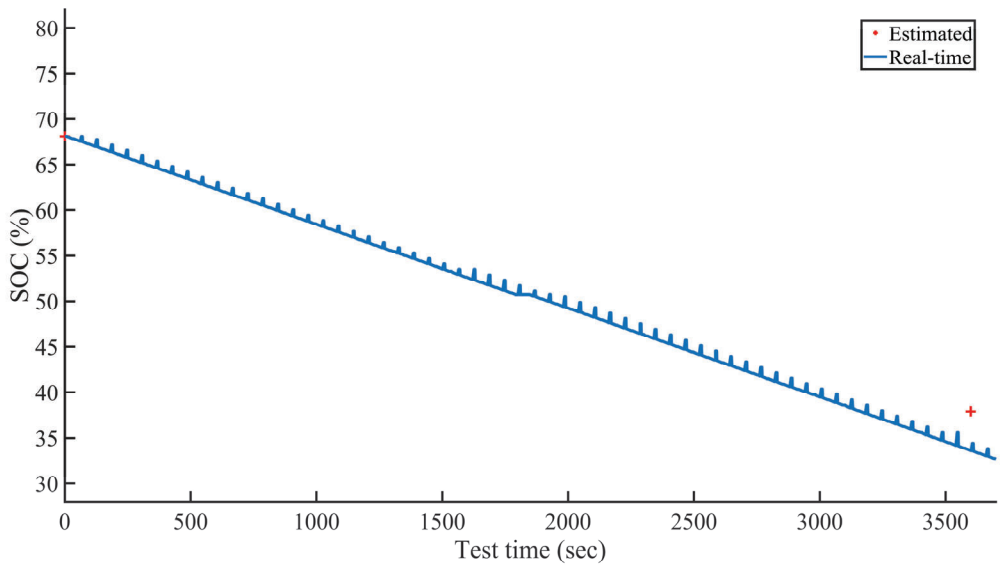

Figure 50 : The estimated SOC and the real-time value of SOC (updated per 5 sec) of HSBLL BESS (DemoCase2).

Performance metrics of the demonstration can be seen in Table 10, where the "-" sign means that the buildings decrease their imported power.

Table 10 : Performance metrics of DemoCase2

	HSB LL	Brf Viva
Estimated SOC after flexibility dispatch	37.91 %	31.02 %
Actual SOC after flexibility dispatch	33.58 %	32.84 %
Flexibility amount	-3 kW	-29 kW
Requested price per kW	0.0560	0.0597

6. Conclusions and future work

The compatibility of the battery models with the actual system behaviour was demonstrated on 5min, 15min and hourly time-scales. The results in Brf Viva revealed that the BESS has been following the charging/discharging power commands with a negligible deviation. The demonstration results also matched the simulation results. The results in HSB LL also showed very good response, when certain limitations in delivered charging power were considered. If those limitations are not considered, then the ideal BESS should not be used. The value of using a non-ideal data-driven model was more evident in the HSB LL BIMG. Regarding the SOC estimation of the models that were considered appropriate for implementation, 5min and 15min time-scales work well enough. Hourly battery scheduling should be avoided.

The tests carried out in this study focused primarily on validating the accuracy of the battery models for energy management implementations. Several factors may influence the results and the expected costs of the applied battery operation strategy. It is essential to incorporate forecast models in the energy management system to forecast the load, the PV generation, and the energy price with small errors to obtain accurate cost estimation as a result of implementing energy management algorithms. Moreover, the battery degradation models and the considered battery stress factors and degradation parameters also influence the results. These models may vary for each specific battery type.

The demonstration at the Brf Viva buildings was only possible after deactivating the maintenance mode of the batteries. If the maintenance mode is kept exactly as it is, then it introduces a great uncertainty in the behaviour of the battery system, making it very difficult to model-perhaps a forecasting model should be used to model the battery in that case.

The demonstration results, which validated the BES models, proved that the proposed energy management strategies can be very useful for the BIMG operator. The energy management strategies can be employed for real-time control of the resources in BIMGs to reduce the expected energy cost in short-term. Moreover, they can be used in long-term studies to determine the optimal battery sizing or define which operation strategy is more appropriate to reduce the building cost. The BIMG owner can opt to minimize the cost through energy arbitrage and therefore frequently cycle the BESS within a day or follow a more conservative approach to avoid battery degradation.

Acknowledgement

I would like to acknowledge the help and technical support of Per Axelson (Ferroamp) and Joachim Högfeldt (Volvo) during the tests in Brf Viva. I would also like to thank Helena Nordström (Göteborg

Energi) and Ylva Olofsson (Volvo) for coordinating the Brf Viva tests. Finally, I would like to thank Anders Becker, Wasif Adnan and Ted Houbaer from Ferroamp for their prompt action in providing significant, last-minute technical support with HSB LL battery.

References

[1] D. Y. Yamashita, I. Vechiu, and J.-P. Gaubert, "A review of hierarchicalcontrol for building microgrids," Renewable and Sustainable Energy Reviews, vol. 118, p. 109523, Feb. 2020.

[2] H. Fontenot and B. Dong, "Modeling and control of building-integrated microgrids for optimal energy management–A review," Applied Energy, vol. 254, p. 113689, Nov. 2019.

[3] HSB, "HSB living lab." [Online]. Available: https://www.hsb.se/hsblivinglab/

[4] K. Antoniadou-Plytaria, A. Srivastava, M. A. F. Ghazvini, D. Steen, L. A. Tuan and O. Carlson, "Chalmers campus as a testbed for intelligent grids and local energy systems," in *Proc. Int. Conf. Smart Energy Syst. Technol. (SEST),* Porto, Portugal, Sep. 2019.

[5] https://ferroamp.com/sv/

[6] https://www.riksbyggen.se/ny-bostad/aktuella-projekt/vastra-gotaland/brf-viva/

[7] K. Antoniadou-Plytaria, "Report on physical micro-grid interface with real test-site validation– report for m2M-GRID project," 2019. [Online]. Available: https://m2m-grid.eu/results/

[8] I. E. Grossmann, "Review of nonlinear mixed-integer and disjunctive programming techniques," Optimization and Eng., vol. 3, no. 3, pp. 227-252, Sep. 2002.

[9] A. J. Gonzalez-Castellanos, D. Pozo, and A. Bischi, "Non-ideal linear operation model for li-ion batteries," *IEEE Trans. on Power Syst.*, vol. 35, no. 1, pp. 672–682, Jan. 2020.

[10] M. A. Ortega-Vazquez, "Optimal scheduling of electric vehicle charging and vehicle-to-grid services at household level including battery degradation and price uncertainty," IET Gen., Transm. & Dis., vol. 8, no. 6, pp. 1007–1016, June 2014.

[11] http://mqtt.org/

[12] K. Antoniadou-Plytaria, D. Steen, L.A. Tuan, and O. Carlson. "Energy scheduling strategies for grid-connected microgrids: A case study on Chalmers campus," in *Proc. IEEE PES Innovative Smart Grid Technologies Europe (ISGT-Europe)*, Bucharest, Romania, Oct. 2019.

[13] IEEE Guide for Loading Mineral-Oil-Immersed Transformers and Step-Voltage Regulators," in IEEE Std C57.91-2011 (Revision of IEEE Std C57.91-1995) , vol., no., pp.1-123, 7 Mar. 2012.